Int. J. Solids Structures, 1968, Vol. 4, pp. 243 to 286. Pergamon Press. Printed in Great Britain

MOVING STEP LOAD ON THE SURFACE OF A HALF-SPACE OF GRANULAR MATERIAL*

H. H. BLEICH

Director Institute of Flight Structures, Columbia University, New York, N.Y.

and

A. T. MATTHEWS and J. P. WRIGHT

P. Weidlinger, New York, N.Y.

NOTATION†

$b_{1,\ldots,9}$	functions defined by equations (31), (38), (157) and (158)
c_P, c_S, $\bar{c}$	velocity of propagation of elastic P-waves, S-waves, and inelastic shock fronts, respectively
E	Young's modulus
F	plastic potential, equation (4)
G	shear modulus
J_1, J_2	invariants, equations (2) and (3)
$K = \dfrac{2(1+\nu)}{3(1-2\nu)}G$	bulk modulus
$L < 0$	function related to inelastic behavior, equation (28)
$p(x-Vt)$	surface pressure
p_0	intensity of step pressure
R	ratio of principal stresses
s_1, s_2	principal stress deviators
s_x, s_y, s_N, s_T, s_{ij}	stress deviators with respect to axes x, y, etc.
t	time
$\dot{u}$, $\dot{v}$	particle velocities in x and y directions, respectively
$\dot{u}_N$, $\dot{u}_T$	normal and tangential component of particle velocities, respectively
U	characteristic velocity
V	velocity of surface pressure
x, y	Cartesian coordinates, Fig. 1
$X = \dfrac{\rho V^2}{2G}\sin^2\varphi$	nondimensional expression
X_P, X_S	values of X at P- and S-fronts, respectively
α	material parameter related to the angle of internal friction, equation (126)
$\beta = \dfrac{s_1-s_2}{s_1+s_2}$	nondimensional stress variable
γ	angle between σ_1 and position ray of element, Fig. 4
δ	angle between σ_1 and normal to S-front
$\Delta \equiv \beta-3$	small quantity for purposes of asymptotic expansion
$\Delta\sigma$, $\Delta\dot{u}$, etc.	increments of σ, $\dot{u}$, etc., at a front
$\varepsilon \equiv \varphi-\bar{\varphi}$	small quantity for purposes of asymptotic expansion
ε_{ij}, $\dot{\varepsilon}_{ij}$	strain, strain rates
$\dot{\varepsilon}^E_{ij}$, $\dot{\varepsilon}^P_{ij}$	elastic and inelastic strain rates, respectively
$\eta \equiv \gamma-\dfrac{\pi}{2}$	small quantity for purposes of asymptotic expansion

* The paper contains results of research sponsored by the Air Force Weapons Laboratory, Kirtland Base, N.M., with P. Weidlinger, Cons. Engineers.

† Other symbols, which are used in one location only, are defined as they occur.

θ	angle defining the direction of the major principal stress, Fig. 4
$\lambda > 0$	function related to inelastic behavior, equation (10)
$\mu = \dfrac{\alpha^2 J_1}{s_1 + s_2}$	nondimensional stress variable
ν	Poisson's ratio
$\pi = 3{\cdot}14159\ldots$	
ρ	mass density of medium
$\sigma_{ij}, \dot{\sigma}_{ij}$	stresses, stress rates
$\sigma_1, \sigma_2, \sigma_3$	principal stresses
τ	shear stress
φ	position angle of element, Fig. 4
$\varphi_P, \varphi_S, \bar{\varphi}$	position of elastic P- and S- and inelastic shock fronts, respectively
φ_1, φ_2, etc.	limits of inelastic regions
Φ	angle of internal friction
$'$	differentiation with respect to φ

Abstract—The two-dimensional steady-state problem of the effect of a step pressure traveling with superseismic velocity on the surface of a half-space is treated for an elastic–plastic material. The plasticity condition selected is a function of the first and second invariants of the stress tensor, and is suitable for a granular medium where inelastic deformations are due to internal slip subject to Coulomb friction.

The problem is inherently nonlinear and leads to a system of coupled nonlinear differential equations which are solved by digital computer. The character of the solutions is radically dependent on the significant non-dimensional parameters, i.e. the Mach number, Poisson's ratio and a value α defining the angle of internal friction. A table giving the solutions for various combinations of the parameters is given.

1. INTRODUCTION

THE two dimensional problem of the effect of a pressure pulse $p(x-Vt)$ progressing with the velocity V on the surface of an elastic half-space, Fig. 1, has been treated by Cole and Huth [1] for a line load and, by superposition, may be found for any other distribution $p(x-Vt)$. Miles [2] has considered the three dimensional problem of loads with axially symmetric distribution $p(r, t)$ over an expanding circular area on the surface, Fig. 2. He has demonstrated that the plane problem [1] contains the asymptotic solution for the three dimensional problem [2] in the region near the wave front. The actual solution of the three dimensional problem would require a great numerical effort, which can be avoided by using the solution of the plane problem to estimate the effect of circularly expanding surface loads.

Real materials can not be expected to be elastic, and solutions of the three-dimensional problem, Fig. 2, for dissipative materials are extremely complex. However, estimates for the three-dimensional case can be made from generalizations of the problem treated in [1] for dissipative materials. This has been done for linearly viscoelastic materials [3] and [4], in the superseismic and subseismic ranges, respectively. The superseismic case for an elastic–plastic material subject to the von Mises yield condition has recently been treated [5] by two of the authors. For possible application to granular media the present paper considers an alternative material where internal slip subject to Coulomb friction may occur.

The slip mechanism in the medium makes the problem nonlinear, so that superposition is not permitted and each pressure distribution $p(x-Vt)$ poses a separate problem. The present paper treats only the case of a progressing step load $p(x-Vt) \equiv p_0 H(Vt-x)$.

Based on concepts of the theory of elastic–plastic materials, it is shown in [6] that an isotropic material subject to internal Coulomb friction can be represented by a model, the behavior of which is governed by a plastic potential

$$F = |\sqrt{J_2}| + \alpha J_1 - k \tag{1}$$

where J_1 and J_2 are the invariants

$$J_1 = \sigma_{ii} \tag{2}$$

$$J_2 = \tfrac{1}{2} s_{ij} s_{ij} \tag{3}$$

while $\alpha > 0$ and $k \geq 0$ are material constants. α is related to the angle of internal friction and is therefore subject to the limit $\alpha < \sqrt{\frac{1}{12}}$, [6], and k is a measure of the cohesion. Because the surface pressures for which this study is intended are large compared to the magnitude of cohesion, only the limiting case $k \to 0$, is considered. Equation (1) then gives

$$F = |\sqrt{J_2}| + \alpha J_1. \tag{4}$$

The effect of the restriction to the limiting case $k \to 0$ is discussed in the Conclusions.

The behavior of the material is described by the following statements:

1. To represent a granular material with no cohesion, the mean stress $J_1/3$ must be compressive, or

$$J_1 \leq 0. \tag{5}$$

2. If, in an element of the material at a given instant,

$$F < 0 \tag{6}$$

the changes in stress and strain, $\dot{\sigma}_{ij}$, $\dot{\varepsilon}_{ij}$ will be related by the conventional elastic relations.

3. However, if the yield condition at a time t is satisfied

$$F = 0 \tag{7}$$

three possibilities exist. There may be further loading of the element with permanent plastic deformation and dissipation of energy, in which case $\dot{F} = 0$. Alternatively, there may be unloading without permanent deformation, in which case $\dot{F} < 0$. Finally, there may be a neutral state, where $\dot{F} = 0$, but no permanent deformation or energy dissipation occurs. If plastic deformations occur, the total strain rate will be the sum of an elastic and a plastic portion

$$\dot{\varepsilon}_{ij} = \dot{\varepsilon}^E_{ij} + \dot{\varepsilon}^P_{ij} \tag{8}$$

where $\dot{\varepsilon}^E_{ij}$ is obtained from the conventional elastic relations, while

$$\dot{\varepsilon}^P_{ij} = \lambda \frac{\partial F}{\partial \sigma_{ij}}\,. \tag{9}$$

The quantity λ, which must be positive,

$$\lambda > 0 \tag{10}$$

is an *a priori* unknown function of space and time. In case of unloading, and in the neutral case the elastic stress–strain relations

$$\dot{\varepsilon}_{ij} = \dot{\varepsilon}^{E}_{ij} \tag{11}$$

apply. The neutral case occurs in the solutions obtained later in regions where $\dot{\varepsilon}_{ij} \equiv \dot{\sigma}_{ij} \equiv 0$.

The fact that the same set of differential equations does not hold everywhere, but that there are regions with moving, *a priori* unknown boundaries, complicates the solution of dynamic problems in this type of material considerably. In the following, the basic equations will be formulated separately in regions with and without additional permanent deformations at the particular time t, and the solutions will be matched to obtain a complete solution satisfying the prescribed surface conditions. The problem being much too complex to expect closed solutions, a numerical approach suitable for digital computers will be employed. The technique is related to the theory of characteristics and is a generalization of the method used in [7].

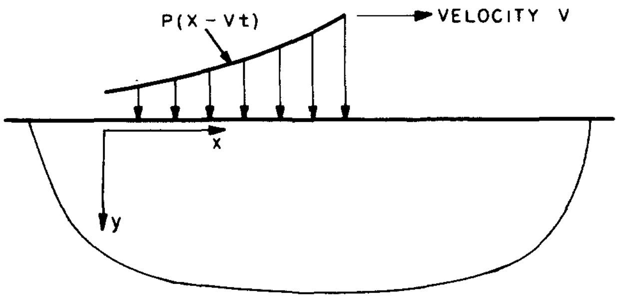

FIG. 1

The problem to be solved considers only the steady-state, i.e. the fact is ignored that in reality the loads $p(x-Vt)$ in Fig. 1 must have begun at some large but finite negative value of time. This omission of the initial condition results in a lack of uniqueness, which can be removed by consideration of the character of solutions of the problem in Fig. 2.

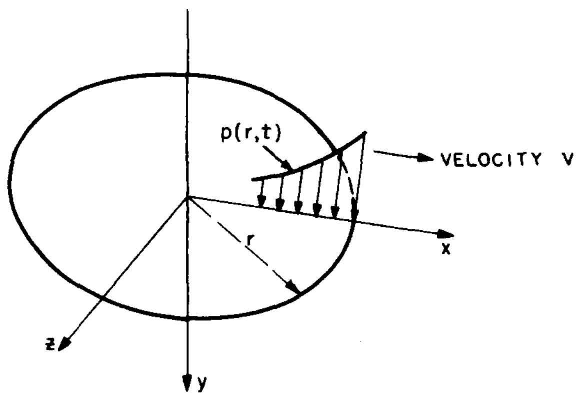

FIG. 2

The lack of uniqueness and a remedy are best seen in the elementary example of a half-space of an inviscid compressible fluid loaded by a uniform pressure pulse, p, which progresses with supersonic velocity, $V > c$. There is an obvious solution, Fig. 3a, in which the load produces a plane wave of intensity p progressing with a front inclined at the appropriate angle $\psi = \sin^{-1} c/V$. However, this is not the only steady-state solution. An alternative is a plane wave, the front of which is inclined at the angle $180° - \psi$. Combinations of the two solutions are also correct steady-state solutions. To find states generated by the application of pressure on the surface only, it can be reasoned that solutions which include the wave front shown in Fig. 3b can not apply because the medium ahead of the front shown in Fig. 3a should be undisturbed when the applied load moves with supersonic velocity. Thus, in case of the fluid a unique solution is obtained. Similar reasoning will be used in the present problem.

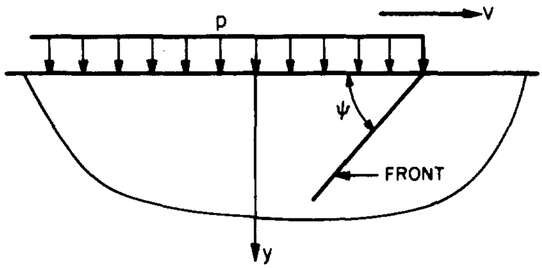

FIG. 3a

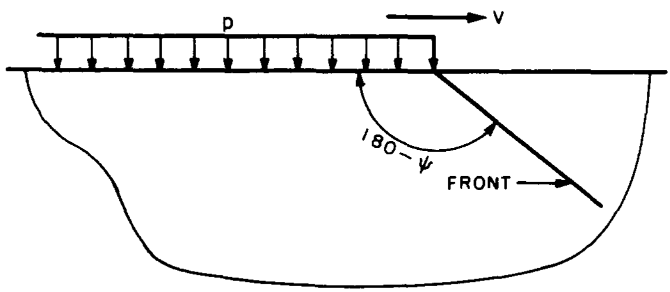

FIG. 3b

2. FORMULATION OF THE BASIC EQUATIONS

Figure 4 indicates the half-space and a system of Cartesian coordinates. x is in the direction of motion of the step load, y and z are normal to the surface in and out of the plane of the paper, respectively. The analysis considers the case of plane strain, $\varepsilon_z = 0$, when the velocity of V of the step load is superseismic, i.e. larger than the velocity of elastic P-waves in the material. Throughout the analysis it is assumed that the strains and velocities are small.

As stated in the introduction there are, in general, inelastic regions in space–time where additional permanent deformations occur, and other regions where changes of stress and

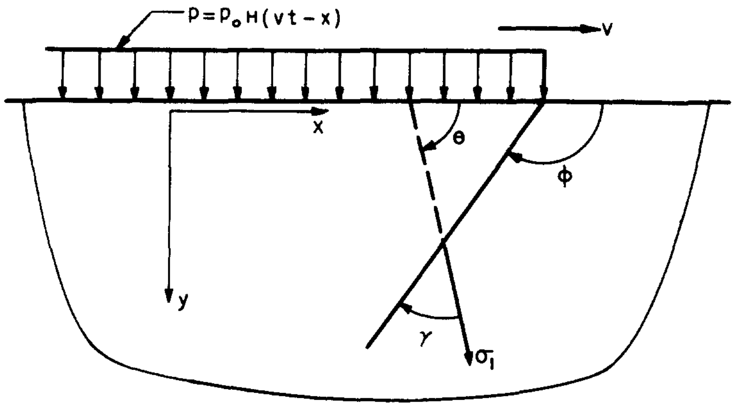

FIG. 4

strain are entirely elastic. The basic differential equations for the two types of region must be treated separately. It will also be necessary to consider the possibility of shock fronts, where the differential equations break down.

2.1 *Inelastic regions*

Combining the familiar stress–strain relation

$$\dot{\varepsilon}_{ij}^{E} = \frac{1+\nu}{E}\left[\dot{\sigma}_{ij} - \frac{\nu}{1+\nu}\delta_{ij}\dot{\sigma}_{kk}\right] \tag{12}$$

where δ_{ij} is the Kroneker delta, and the relation

$$\dot{\varepsilon}_{ij} = \frac{1}{2}[\dot{u}_{i,j} + \dot{u}_{j,i}] \tag{13}$$

gives, for plane strain, four constitutive equations

$$\frac{\partial \dot{u}}{\partial x} = \frac{1}{E}[\dot{\sigma}_{xx} - \nu(\dot{\sigma}_{yy} + \dot{\sigma}_{zz})] + \lambda\frac{\partial F}{\partial \sigma_{xx}} \tag{14}$$

$$\frac{\partial \dot{v}}{\partial y} = \frac{1}{E}[\dot{\sigma}_{yy} - \nu(\dot{\sigma}_{xx} + \dot{\sigma}_{zz})] + \lambda\frac{\partial F}{\partial \sigma_{yy}} \tag{15}$$

$$0 = \frac{1}{E}[\dot{\sigma}_{zz} - \nu(\dot{\sigma}_{yy} + \dot{\sigma}_{xx})] + \lambda\frac{\partial F}{\partial \sigma_{zz}} \tag{16}$$

$$\frac{\partial \dot{u}}{\partial y} + \frac{\partial \dot{v}}{\partial x} = \frac{1}{G}\dot{\tau} + \lambda\frac{\partial F}{\partial \tau} \tag{17}$$

where $\dot{u}$ and $\dot{v}$ are, respectively, the x and y components of the particle velocity. Further, in a linear theory the two equations of motion are

$$\frac{\partial \sigma_{xx}}{\partial x} + \frac{\partial \tau}{\partial y} = \rho\frac{\partial \dot{u}}{\partial t} \tag{18}$$

$$\frac{\partial \tau}{\partial x} + \frac{\partial \sigma_{yy}}{\partial y} = \rho\frac{\partial \dot{v}}{\partial t}. \tag{19}$$

The yield condition, equation (4), and equations (14)–(19) form a set of seven equations governing inelastic regions. Inherently, however, the unknown function λ must satisfy the inequality $\lambda > 0$, equation (10), required for an element in an inelastic region.

It was found convenient to express the four unknown stresses by four other variables, viz. the invariant J_1, the two principal stress deviators s_1 and s_2, and the angle θ formed by the direction of s_1 with the surface, Fig. 4. The appropriate relations are

$$\sigma_{xx} = s_2 \sin^2 \theta + s_1 \cos^2 \theta + \tfrac{1}{3} J_1 \tag{20}$$

$$\sigma_{yy} = s_1 \sin^2 \theta + s_2 \cos^2 \theta + \tfrac{1}{3} J_1 \tag{21}$$

$$\sigma_{zz} = -s_1 - s_2 + \tfrac{1}{3} J_1 \tag{22}$$

$$\tau = \frac{\sigma_1 - \sigma_2}{2} \sin 2\theta. \tag{23}$$

In the numerical analysis the subscripts 1 and 2 will be selected such that s_1 is the major compressive deviator.

Because the steady state case is considered, all quantities appearing in the analysis which are functions of x and t must be of the form $f(x - Vt)$. For the step load $p = p_0 H(Vt - x)$, dimensional considerations similar to those used in [5] make it plausible that the various quantities do not depend on $x - Vt$ and y separately, but must be solely functions of the ratio $(x - Vt)/y$. This permits introduction of the angle ϕ, shown in Fig. 4, as new independent variable,

$$\phi = \cot^{-1} \frac{x - Vt}{y}. \tag{24}$$

This transformation changes the six partial differential equations obtained above into a set of six simultaneous ordinary differential equations. A seventh differential equation is obtained by taking a derivative of the yield condition. By elimination of the velocities $\dot{u}$ and $\dot{v}$, one finally obtains a system of five ordinary differential equations,*

$$\begin{bmatrix} -1 & -1 & \dfrac{1-2\nu}{1+\nu} & 0 & s_1 + s_2 + 2\alpha^2 J_1 \\ \sin^2 \gamma & \cos^2 \gamma & 1 - 3X\left(\dfrac{1-2\nu}{1+\nu}\right) & -\sin 2\gamma & -6X\alpha^2 J_1 \\ \tfrac{1}{2}\sin 2\gamma & \tfrac{1}{2}\sin 2\gamma & \sin 2\gamma & 2X - 1 & 0 \\ \sin^2 \gamma - X & X - \cos^2 \gamma & -\cos 2\gamma & 0 & X(s_1 + s_2) \\ 2s_1 + s_2 & s_1 + 2s_2 & -6\alpha^2 J_1 & 0 & 0 \end{bmatrix} \begin{bmatrix} s_1' \\ s_2' \\ \tfrac{1}{3} J_1' \\ (s_1 - s_2)\theta' \\ \dfrac{GL}{V} \end{bmatrix} = 0 \tag{25}$$

* Details of the manipulations may be found in [8].

where

$$\gamma = \varphi - \theta \tag{26}$$

$$X = \frac{\rho V^2}{2G} \sin^2 \varphi \tag{27}$$

$$L = +\frac{\lambda y}{\alpha J_1 \sin^2 \varphi} < 0. \tag{28}$$

The meaning of the angle γ is shown in Fig. 4. The inequality in equation (28) follows from $\lambda > 0$, equation (10), and $J_1 < 0$, equation (5).

The unknowns in the differential equations (25) are four quantities defining the stress field, s_1, s_2, J_1 and θ, and a fifth quantity L which is a measure of the rate of plastic deformation. The set of equations is linear and homogeneous in the four derivatives and in the quantity L, and may be satisfied by

$$s_1' = s_2' = J_1' = (s_1 - s_2)\theta' = L = 0. \tag{29}$$

However, $L = 0$ implies $\lambda = 0$, which violates equation (10). It follows that in an inelastic region the determinant of equations (25) must vanish, giving the "determinantal equation"

$$b_2^2 + b_1 b_3 = 0 \tag{30}$$

where

$$\left.\begin{aligned} b_1 &= 2[1+(1-2X)(1-2\nu)] \\ b_2 &= \beta\cos 2\gamma + (1-2X)[1-2\nu-4\mu(1+\nu)] \\ b_3 &= (1+\nu)(1-2X)(1+2\mu)^2 - \beta^2 X \end{aligned}\right\} \tag{31}$$

and

$$\beta = \frac{s_1 - s_2}{s_1 + s_2} \tag{32}$$

$$\mu = \frac{\alpha^2 J_1}{s_1 + s_2}. \tag{33}$$

Due to the vanishing of its determinant only four of the five equations (25) are independent. As L may not vanish, s_1', s_2', J_1' and θ' can always be expressed in terms of L,

$$s_1' = \tfrac{1}{2}(s_1 + s_2)(b_5 + b_4)\frac{GL}{V} \tag{34}$$

$$s_2' = \tfrac{1}{2}(s_1 + s_2)(b_5 - b_4)\frac{GL}{V} \tag{35}$$

$$\theta' = b_6 \frac{GL}{V} \tag{36}$$

$$J_1' = 3(s_1 + s_2) b_7 \frac{GL}{V} \tag{37}$$

where

$$\left.\begin{aligned} b_4 &= \frac{2}{1-2X}\left[\frac{b_2}{b_1}\cos 2\gamma - \beta X\right] \\ b_5 &= \frac{2}{3}(1+\nu)\left[\frac{1-2\nu}{1+\nu}\frac{b_2}{b_1} + 1 + \alpha\sqrt{(3+\beta^2)}\right] \\ b_6 &= \frac{\sin 2\gamma}{\beta(1-2X)}\frac{b_2}{b_1} \\ b_7 &= \frac{b_2}{b_1} - \frac{b_5}{2}. \end{aligned}\right\} \tag{38}$$

Since equation (30) must remain valid throughout an inelastic region, it may be differentiated with respect to ϕ. Substitution of equations (34)–(37) into this expression furnishes a linear equation for the value of L,

$$\frac{GL}{V} = \frac{\left\{\begin{array}{l} 2Xb_3(1-2\nu)\sin 2\varphi + \frac{1}{2}Xb_1 \sin 2\varphi\,[2(1+\nu)(1+2\mu)^2+\beta^2] + \\ +2b_2[\beta \sin 2y \sin^2\varphi + X\sin 2\varphi\,(1-2\nu) - 4X \sin 2\varphi\,(1+\nu)\mu] \end{array}\right\}}{\left\{\begin{array}{l} b_1[(1+\nu)(1+2\mu)(1-2X)(b_5+6\alpha^2 b_7) - Xb_4\beta] + \\ +b_2[b_4\cos 2y + 2\beta b_6 \sin 2y + b_5(1-2X)(1-2\nu) - \\ -12b_7\alpha^2(1+\nu)(1-2X)] \end{array}\right\}\sin^2\varphi}. \tag{39}$$

The derivatives s_1', s_2', J_1' and θ' can be obtained by substitution of equation (39) into equations (34)–(37).

If the values of s_1, s_2, J_1 and θ are known on one boundary of an inelastic region, their values in the interior of such a region can be found from equations (34) to (39) by forward integration. The starting values of s_1, s_2, J_1 and θ must satisfy the yield condition,

$$s_1^2 + s_1 s_2 + s_2^2 - \alpha^2 J_1^2 = 0 \tag{40}$$

and the determinantal equation, equation (30). Further, the forward integration is permitted only when $L < 0$, as required by equation (28).

2.2 *Inelastic shock fronts*

The analysis in the previous subsection treated regions of finite extent, and the additional possibility of infinitely thin regions, i.e. shock fronts, remains to be considered. If such fronts exist in the present problem the equations obtained above should indicate this by becoming singular, since at least one of the derivatives of the stresses must become infinite at a shock front. Instead of searching for singularities it is better for a physical understanding to demonstrate the existence and properties of shock fronts in general. This general derivation automatically answers the question of stability of the fronts, by proving that a front, where the stress rises with an arbitrarily steep slope, Fig. 5a, will not disperse but propagate without change of slope.

Consider the basic equations (14)–(19), which apply to any type of wave propagation in plane strain. To investigate the possibility of plane pressure waves without shear, the y direction is selected as the direction of propagation. For such a wave, the shear τ, the horizontal velocity $\dot{u}$ and all derivatives with respect to x vanish, while for reasons of

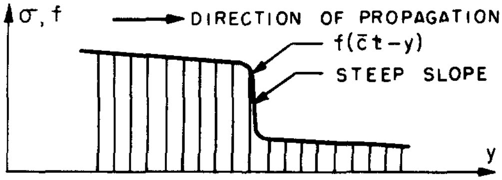

FIG. 5a

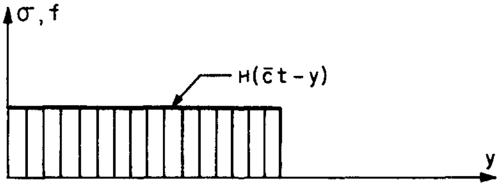

FIG. 5b

symmetry $\sigma_x \equiv \sigma_z$. Since x, y, z are the principal directions, the stress deviators s_x and s_y become $s_x = s_2$, $s_y = s_1$. Using the relation $s_2 = -\frac{1}{2}s_1$, the yield condition (40) becomes

$$\tfrac{3}{4}s_1^2 - \alpha^2 J_1^2 = 0 \tag{41}$$

while equations (14)–(19) furnish three relations

$$\frac{\partial \dot{v}}{\partial y} = \frac{1}{2G}\dot{s}_1 + \frac{1}{9K}\dot{J}_1 + \bar{\lambda}[s_1 - 2\alpha^2 J_1] \tag{42}$$

$$0 = -\frac{1}{4G}\dot{s}_1 + \frac{1}{9K}\dot{J}_1 - \bar{\lambda}[\tfrac{1}{2}s_1 + 2\alpha^2 J_1] \tag{43}$$

$$\rho\frac{\partial \dot{v}}{\partial t} = \frac{\partial s_1}{\partial y} + \frac{1}{3}\frac{\partial J_1}{\partial y} \tag{44}$$

where

$$\bar{\lambda} = -\frac{\lambda}{2\alpha J_1}, \qquad K = \frac{2}{3}G\left(\frac{1+\nu}{1-2\nu}\right). \tag{45}$$

If a steep front, Fig. 5a, at which inelastic deformation occurs, is to propagate with a velocity $\bar{c}$ without change of slope, it is necessary that

$$s_1 = a_1 f(y - \bar{c}t) = a_1 f(\zeta) \tag{46}$$

$$J_1 = a_2 f(y - \bar{c}t) = a_2 f(\zeta) \tag{47}$$

$$\dot{v} = a_3 f(y - \bar{c}t) = a_3 f(\zeta) \tag{48}$$

where $\zeta = y - \bar{c}t$, while the values a_i and $\bar{c}$ are free constants, and f is an arbitrary function. Since J_1 is necessarily negative, and the signs of the coefficients a_i are still undefined, one can select the sign of f without loss of generality, say

$$f > 0. \tag{49}$$

The increase of $|f|$ with time requires then

$$f' < 0 \tag{50}$$

where the symbol $'$ indicates derivatives with respect to ζ.

Substituting equations (46)–(48) into equations (41)–(44) and eliminating the velocity $\dot{v}$ yields

$$f'\left[a_1\left(1-\frac{\rho\bar{c}^2}{2G}\right)+\frac{1}{3}a_2\left(1-\frac{\rho\bar{c}^2}{3K}\right)\right]+\rho\bar{c}\bar{\lambda}f\left[a_1-2\alpha^2a_2\right]=0 \tag{51}$$

$$f'\left[\frac{1}{2}\frac{\rho\bar{c}^2}{2G}a_1-\frac{1}{3}\frac{\rho\bar{c}^2}{3K}a_2\right]-\rho\bar{c}\bar{\lambda}f\left[\frac{1}{2}a_1+2\alpha^2a_2\right]=0 \tag{52}$$

$$f^2\left[\frac{3}{4}a_1^2-\alpha^2a_2^2\right]=0. \tag{53}$$

If shock fronts of the type sought exist, these three equations must be satisfied for arbitrary functions f, subject to the limitations of equations (49), (50) and subject to the condition $\bar{\lambda} > 0$. Equation (53) gives

$$\frac{a_2}{a_1}=\pm\frac{\sqrt{3}}{2\alpha}. \tag{54}$$

Equations (51) and (52) permit nonvanishing values f, $\bar{\lambda}$ and f' only if the determinant of the coefficients of f' and $\rho\bar{c}\bar{\lambda}f$ vanishes, yielding after substitution of equation (54)

$$\bar{c}^2=\frac{K}{\rho}\frac{(1\pm 2\alpha\sqrt{3})^2}{\left[1+6\alpha^2\left(\frac{1+\nu}{1-2\nu}\right)\right]}. \tag{55}$$

However, the result is valid if, and only if, $\bar{\lambda} > 0$. Computing $\bar{\lambda}$ from equation (51) yields, after simple manipulations, the inequality

$$1\mp\frac{1}{\sqrt{3}}\frac{1-2\nu}{\alpha(1+\nu)}<0 \tag{56}$$

where the upper or lower signs in equations (54)–(56) are to be used consistently. The limitations $\alpha > 0$ and $0 \le \nu < \frac{1}{2}$ indicate that the lower sign never leads to a valid solution. Using the upper sign one obtains the requirement

$$\alpha<\frac{1}{\sqrt{3}}\frac{1-2\nu}{1+\nu} \tag{57}$$

and the corresponding velocity

$$\bar{c}^2=\frac{K}{\rho}\frac{(1+2\alpha\sqrt{3})^2}{\left[1+6\alpha^2\left(\frac{1+\nu}{1-2\nu}\right)\right]}. \tag{58}$$

The stresses s_1 and J_1 at the front have the ratio

$$\frac{s_1}{J_1} = \frac{a_1}{a_2} = \frac{2\alpha}{\sqrt{3}}. \tag{59}$$

The function f being arbitrary, it may be selected as a step function,

$$f(y-\bar{c}t) = H(\bar{c}t-y) \tag{60}$$

as shown in Fig. 5b. The discontinuities Δs_1 and ΔJ_1 in the stress history

$$s_1 = \Delta s_1 H(\bar{c}t-y) \tag{61}$$

$$J_1 = \Delta J_1 H(\bar{c}t-y) \tag{62}$$

then satisfy equation (59) provided

$$\frac{\Delta s_1}{\Delta J_1} = \frac{2\alpha}{\sqrt{3}}. \tag{63}$$

The corresponding velocity to be obtained from equation (48) is

$$\dot{v} = \Delta\dot{v} H(\bar{c}t-y) \tag{64}$$

where

$$\frac{\Delta\dot{v}}{\Delta J_1} = -\frac{1+2\alpha\sqrt{3}}{3\rho\bar{c}}. \tag{65}$$

Equations (61)–(65) give the relations for an inelastic shock front entering a stressless region, a case which will be utilized in the construction of solutions in Section 3.

The above investigation of possible shock fronts was based on the premise that $\tau = 0$. The fact that inelastic shock fronts are impossible when $\tau \neq 0$ is demonstrated in [8, Appendix A], so that the discontinuity described in this section is the only inelastic one to be considered.

Summarizing, it has been demonstrated that, for values of α and ν which satisfy equation (57), a plane pressure discontinuity will propagate with the velocity $\bar{c}$ given by equation (58). In order to occur in the solution of the steady state problem, Fig. 4, the front must be inclined at such an angle $\bar{\varphi}$ that the horizontal component of the velocity $\bar{c}$ equals the velocity V of the load on the surface. The angle is obtained from equation (58),

$$\bar{\varphi} = \pi - \sin^{-1}\left[\frac{1}{V}\sqrt{\left(\frac{K}{\rho}\right)}\frac{(1+2\alpha\sqrt{3})}{\sqrt{\left[1+6\alpha^2\left(\frac{1+\nu}{1-2\nu}\right)\right]}}\right]. \tag{66}$$

The principal stress at the front being normal to the front, requires

$$\gamma = \frac{\pi}{2}, \qquad \theta = \varphi - \frac{\pi}{2} \tag{67}$$

Further, the relation $s_2 = -\frac{1}{2}s_1$ at the front defines the value β, equation (32)

$$\beta = 3{\cdot}0 \tag{68}$$

2.3 *Regions and shock fronts without inelastic deformation*

In a region where at the instant considered no inelastic deformation occurs, the strain rates are defined by the purely elastic relations, equation (11), and the stresses are subject to the inequalities

$$\left.\begin{aligned} F \equiv |[s_1^2+s_1s_2+s_2^2]^{\frac{1}{2}}|+\alpha J_1 \leq 0 \\ J_1 \leq 0. \end{aligned}\right\} \tag{69}$$

In addition, the equations of motion, equations (18), (19) hold. To obtain the differential equations, one could proceed in the same manner as in Section 2.1. However, it is not necessary to do so, because the resulting differential equations must obviously follow from equation (25) by making the following two changes:

(1) The last equation is to be omitted because it represents the yield condition $F = 0$, which does not apply.

(2) To account for the change in the stress strain law from equation (8) to equation (11), $L = 0$ is to be introduced into equations (25).

In this fashion the following four simultaneous differential equations are obtained.

$$\begin{bmatrix} -1 & -1 & \dfrac{1-2\nu}{1+\nu} & 0 \\ \sin^2\gamma & \cos^2\gamma & 1-3X\left(\dfrac{1-2\nu}{1+\nu}\right) & -\sin 2\gamma \\ \sin 2\gamma & \sin 2\gamma & 2\sin 2\gamma & -2(1-2X) \\ \sin^2\gamma - X & X-\cos^2\gamma & -\cos 2\gamma & 0 \end{bmatrix} \begin{bmatrix} s_1' \\ s_2' \\ \frac{1}{3}J_1' \\ (s_1-s_2)\theta' \end{bmatrix} = 0. \tag{70}$$

The equations are linear and homogeneous so that the derivatives of the stresses, s_1', s_2', J_1' vanish, unless the determinant of equations (70) equals zero. In spite of the fact that the coefficients in equations (70) contain γ, the value of the determinant is independent of this value. The determinant of equations (70) vanishes when X is a root of

$$4X(1-2X)[1+(1-2X)(1-2\nu)] = 0. \tag{71}$$

Equation (71) has two significant roots,

$$X_P = \frac{1-\nu}{1-2\nu} \tag{72}$$

and

$$X_S = \tfrac{1}{2}, \tag{73}$$

and one, $X = 0$, which may be shown to be trivial. Substituting the two roots X_P and X_S into equation (27) furnishes two locations

$$\varphi_P = \pi - \sin^{-1}\left\{\frac{1}{V}\sqrt{\left[\frac{2G}{\rho}\left(\frac{1-\nu}{1-2\nu}\right)\right]}\right\} \equiv \pi - \sin^{-1}\left[\frac{c_P}{V}\right] \tag{74}$$

$$\varphi_S = \pi - \sin^{-1}\left[\frac{1}{V}\sqrt{\left(\frac{G}{\rho}\right)}\right] \equiv \pi - \sin^{-1}\left[\frac{c_S}{V}\right] \tag{75}$$

at which the determinant of equations (70) vanishes, where c_P, c_S are the velocities of P- and S-waves, respectively. In any location $\phi \neq \phi_P$ or ϕ_S the derivatives s_1', s_2', J_1' vanish, so that the stresses must remain constant everywhere, except at the locations ϕ_P and ϕ_S.

The angles ϕ_P and ϕ_S are the locations of potential elastic P- and S-fronts, which may, therefore, be part of the complete solutions to be obtained in Section 3. The following pertinent details for these fronts will be required subsequently.

2.3.1 *The P-front.* Designating the changes in the various quantities at the front by the symbol Δ, the discontinuities in the stresses σ_N, $\sigma_T = \sigma_z$ (normal and tangential to the front, respectively) and in the component $\dot{u}_N$ of the velocity (normal to the front) are proportional,

$$\Delta\sigma_N : \Delta\sigma_T : \Delta\dot{u}_N = 1 : \frac{\nu}{1-\nu} : \frac{-1}{\rho c_P}. \tag{76}$$

No other discontinuities can occur.

The changes $\Delta\sigma_N$ and $\Delta\sigma_T$ are of course restricted by the fact that the inequalities (69) for the stresses must be satisfied on either side of the front. No general study of this restriction is required, but in Section 3 it will be necessary to know if a P-front is possible when the stresses and velocities ahead of the front φ_P vanish. In this case the conditions (69) are satisfied ahead of the front, $F \equiv J_1 \equiv 0$. To check behind the shock, it is noted that the stresses $\Delta\sigma_N$ and $\Delta\sigma_T$ are not only the total stresses, but they are also the principal stresses, $\Delta\sigma_N = \sigma_1$, $\Delta\sigma_T = \sigma_2$. After computation of s_1 and J_1, one finds two necessary conditions for a P-front

$$\sigma_1 < 0 \tag{77}$$

$$\alpha \geq \frac{1}{\sqrt{3}}\frac{1-2\nu}{1+\nu}. \tag{78}$$

A compressive shock front of arbitrary strength $\sigma_1 < 0$ in the location $\varphi = \varphi_P$ is therefore possible if, and only if, the inequality (78) on α is satisfied. The angle γ and the quantity β, equation (32), immediately following the front are

$$\gamma = \frac{\pi}{2}, \qquad \beta = 3. \tag{79}$$

Attention is drawn to the fact that the inequalities (78) and (57) which permit, respectively, an elastic or an inelastic pressure discontinuity to enter a stress free region, are mutually exclusive, but complementary. In other words, for any combination of α and ν, one, but only one, of the two types of fronts can exist.

2.3.2 *The S-front.* At an S-front discontinuities occur only in the shear stress $\tau_N = \tau_T = \tau$ and in the tangential velocity $\dot{u}_T$. The changes are proportional,

$$\Delta\tau : \Delta\dot{u}_T = 1 : \frac{1}{\rho c_S}. \tag{80}$$

In addition, the inequalities (69) must again be satisfied ahead of and behind the front. Checking the situation if the region ahead of the front is stress free, equations (69) are again satisfied ahead of the front. Behind the front the stresses are

$$\tau = \Delta\tau, \qquad \sigma_N \equiv \sigma_T \equiv s_N \equiv s_T \equiv J_1 \equiv 0. \tag{81}$$

The invariant J_2 may be written

$$J_2 = s_N^2 + s_N s_T + s_T^2 + 4\tau^2 \tag{82}$$

and, because in this last equation all stresses, except τ, vanish, the condition

$$F \equiv J_2 - \alpha^2 J_1^2 \leq 0 \tag{83}$$

is violated. Thus an S-front can not enter a stress-free region.

Some details about S-front locations where stresses ahead of the front do not vanish will be required. Consider specifically the possibility of such a front at a point where the equal sign in the first condition (69) applies ahead of the front,

$$F \equiv J_2 - \alpha^2 J_1^2 = 0. \tag{84}$$

This indicates that the material is at the verge of inelastic deformation.

Let the shear stresses just ahead of the front, for $\varphi_S^{(-)}$, be $\bar{\tau}$, and those behind the front, for $\varphi_S^{(+)}$, be τ. The invariant J_1 and the deviators with respect to the N and T directions, s_N and s_T, respectively, are equal at $\varphi_S^{(-)}$ and $\varphi_S^{(+)}$. Noting that the equality (84) is satisfied ahead of the front, it is clear that the inequality equation (83) requires

$$|\tau| \leq |\bar{\tau}|. \tag{85}$$

The largest possible change $\Delta\tau = \tau - \bar{\tau}$ occurs therefore when $\tau = -\bar{\tau}$, in which case equation (84) is satisfied also for $\varphi_S^{(+)}$. It is useful to consider this case in terms of the principal stress variables used in Section 2.1, i.e. using the angle γ and the quantities J_1, s_i and β as variables. Figure 6 shows the direction of the major deviator $\bar{s}_1$ ahead of the

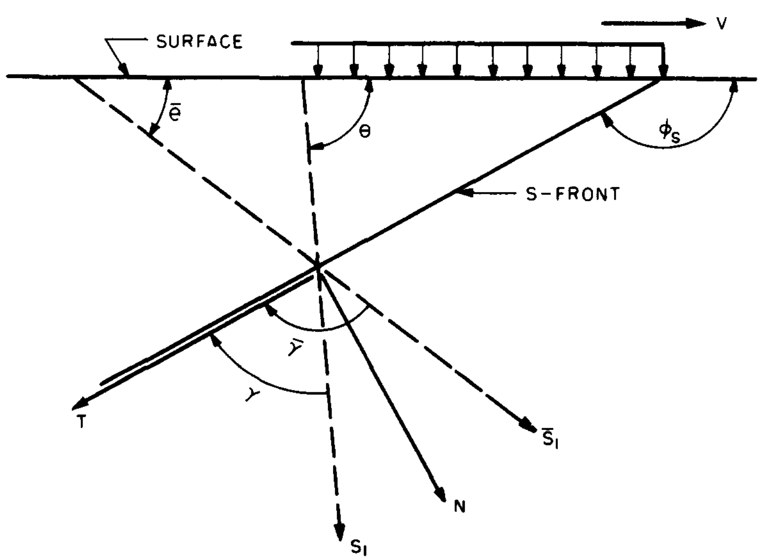

FIG. 6

front at an angle $\bar{\gamma}$ to the S-front. The state of stress ahead of the front, $\bar{\gamma}$, $\bar{s}_1$ and $\bar{s}_2$, corresponds to the values of $\bar{\tau}$, s_N and s_T which apply in this location. Behind the front the state of stress is defined by $\tau = -\bar{\tau}$, s_N, s_T, which stresses define changed values γ, s_1,

s_2. When computing these values by the conventional relations it is found that s_1, s_2, being even functions of τ, are necessarily equal to $\bar{s}_1$, $\bar{s}_2$, respectively. γ, being an odd function of τ, changes

$$\gamma = \pi - \bar{\gamma}. \tag{86}$$

Therefore, a change in shear from $\bar{\tau}$ to $\tau = -\bar{\tau}$ at φ_S does not change the values of the variables s_1, s_2, J_1 or β, but only the values of the angles γ and θ. The latter becomes

$$\text{at } \varphi_S^{(+)}: \qquad \theta = \varphi_S - \gamma = \varphi_S + \bar{\gamma} - \pi. \tag{87}$$

These changes in γ or θ occur if the stresses satisfy the equality (84) ahead of, and behind the front.

3. CONSTRUCTION OF SOLUTIONS

In Section 2 a number of partial solutions were obtained from which the solution of the complete boundary value problem is now to be constructed. Section 2.1 gives the differential equations for the determination of the stresses and velocities in inelastic regions; from Section 2.3 it is known that all unknowns in elastic regions are constants, except for discontinuities of a prescribed nature at the locations φ_S and φ_P. In addition, there may be a shock front with inelastic deformation at a location $\tilde{\varphi}$.

As mentioned in the last two paragraphs of the introduction, steady-state problems of the type studied here need not have unique solutions. However, it may be possible to eliminate excess solutions by specifying that the steady-state solution desired should be the asymptotic solution, if any, of the problem of an expanding load (Fig. 7) applied on a half-space initially at rest. This additional condition is invoked here and furnishes a vital boundary condition for the solution through the reasoning which follows. It is known that the partial differential equations of the transient problem, Fig. 7, are hyperbolic in

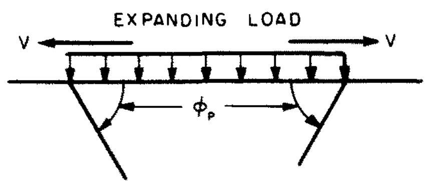

FIG. 7

elastic and in inelastic regions. The characteristic velocities U under elastic conditions are $U = c_P$ and $U = c_S$, while those in the inelastic case are functions of the stresses, but subject to the inequality $U < c_P$. The hyperbolic character of the differential equations and the inequality have been demonstrated in [9] for a general class of elastic–plastic material governed by a plastic potential. This result applies here. The largest characteristic velocity being less than c_P, one can conclude that, in the non-steady-state superseismic problem, $V/c_P > 1$, Fig. 7, all unknowns vanish ahead of a front inclined at an angle ϕ_P corresponding to c_P, so that one has a boundary condition for the steady-state problem

$$\text{for } \phi < \phi_P: \qquad \sigma_i = s_i = \dot{u} = \dot{v} = 0. \tag{88}$$

Additional boundary conditions apply at the loaded surface where the pressure $p_0 H(Vt-x)$ is applied. At this surface one of the two principal stresses must be vertical and equal to $-p_0$, so that there are two alternative boundary conditions. Either

$$\sigma_1 = s_1 + \tfrac{1}{3}J_1 = -p_0, \qquad \gamma = \frac{\pi}{2} \tag{89}$$

or

$$\sigma_2 = s_2 + \tfrac{1}{3}J_1 = -p_0, \qquad \gamma = 0, \pi. \tag{90}$$

It is easily seen that the nature of all equations in Section 2 is such that p_0 will appear as an external factor in the solutions for the stresses and velocities, while the non-dimensional quantities θ, β and γ are independent of p_0. This simplification is due to the homogeneous nature of the plastic potential, equation (4), and would not apply if equation (1), allowing for cohesion, is specified. Therefore, only the case $p_0 = 1$ need be considered, so that equations (89), (90) become

$$\sigma_1 = s_1 + \tfrac{1}{3}J_1 = -1, \qquad \gamma = \frac{\pi}{2} \tag{91}$$

or

$$\sigma_2 = s_2 + \tfrac{1}{3}J_1 = -1, \qquad \gamma = 0, \pi. \tag{92}$$

At this point it must be stressed that no uniqueness or existence theorem for transient problems is available for elastic–plastic materials. Although the boundary condition (88) eliminates certain excess solutions of the steady-state problem, Fig. 8, which clearly are not asymptotic solutions of the transient problem, Fig. 7, the remaining solutions of the steady-state problem may still not be unique, because the original transient problem may not have a unique solution. In constructing solutions it is therefore vital to consider all conceivable possibilities.

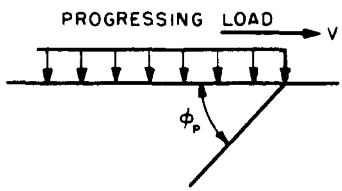

FIG. 8

In the expectation that there should be a continuous transition in character and in the numerical values of the solution, the latter will be considered as functions of the basic physical parameters ν, α and of V/c_P. The concept that the character of the solution should change smoothly as a function of the parameters is extremely helpful in the formulation of the solutions. As a starting point one can explore the existence of a range in the above parameters where the elastic solution applied and from there continue, step by step, into further ranges.

Applying this gradual approach, one arrives at the conclusion that the occurrence of discontinuous fronts at the transition from the stressless to the stressed state in the elastic situation will also apply in the more general case, at least for values of the parameters close to those where the elastic solutions are valid. The first attempt will therefore be the construction of solutions with an initial discontinuity at the arrival time, and the possibility of continuous behavior at arrival will be considered subsequently to demonstrate uniqueness, and also in situations where the assumption of an initial discontinuity does not lead to a solution.

In accordance with the above approach, one expects that the properties of the initial discontinuity will govern the character of the solution as a function of the parameters ν, α and V/c_P. The existence and the nature of the initial discontinuities depend on ν and α only, so that these two parameters play a more important role than V/c_P, and a preliminary classification of the ranges can be based on ν and α only. In the permissible range for these parameters, $0 \leq \nu \leq \frac{1}{2}$ and $0 \leq \alpha \leq 1/\sqrt{12}$, there is according to Section 2.3 a Range 1, Fig. 9a, defined by

$$\sqrt{3}\alpha \geq \frac{1-2\nu}{1+\nu} \tag{93}$$

where an elastic P-front, but no other discontinuity can enter a stress free region, while for

$$\sqrt{3}\alpha < \frac{1-2\nu}{1+\nu} \tag{94}$$

only a compressive discontinuity with inelastic deformation may enter a stress-free region.

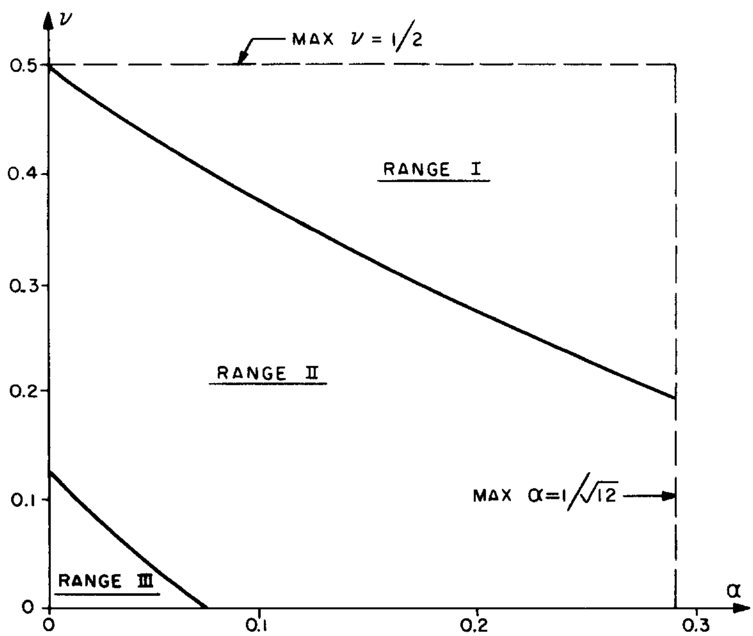

FIG. 9a. Principal ranges.

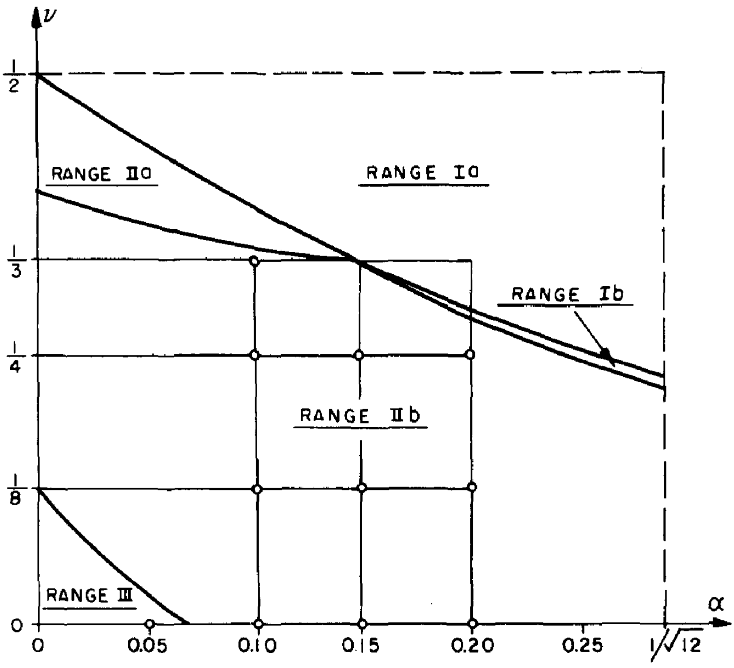

o NUMERICAL RESULTS

FIG. 9b. Subranges for $V/c_P = 5$.

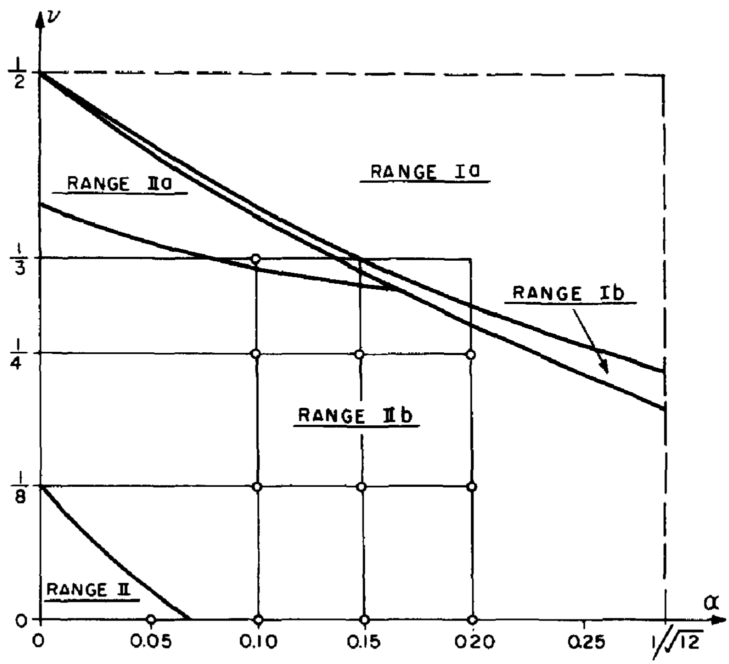

o NUMERICAL RESULTS

FIG. 9c. Subranges for $V/c_P = 2$.

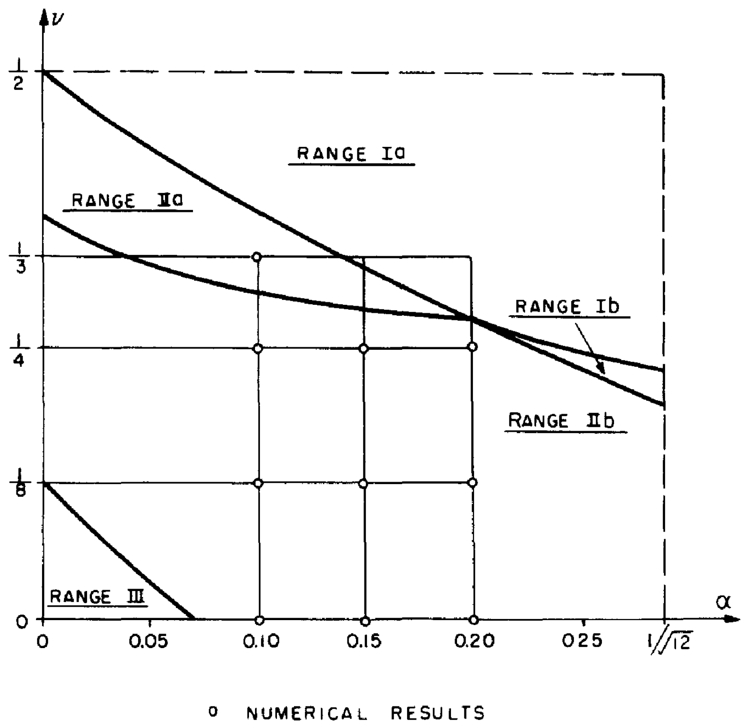

FIG. 9d. Subranges for $V/c_P = 1{\cdot}25$.

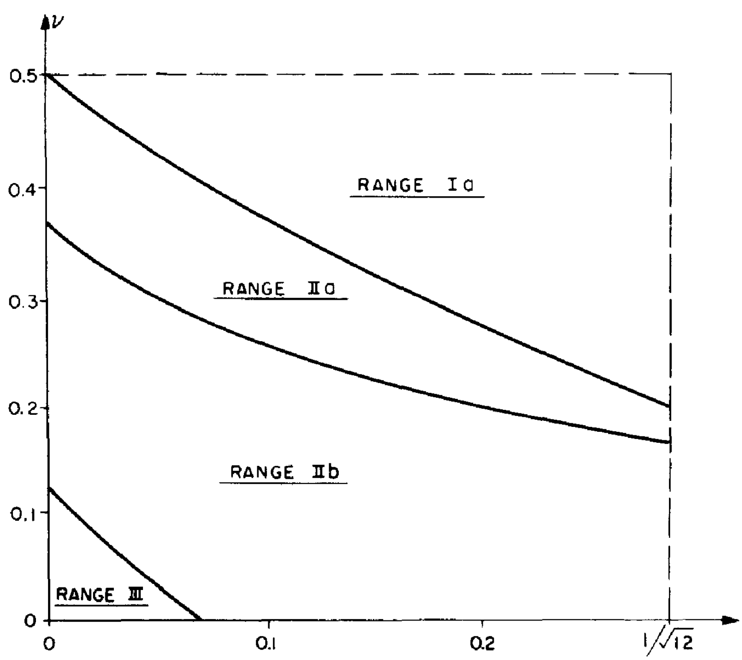

FIG. 9e. Subranges for $V/c_P = 1{\cdot}02$.

The total range where the latter inequality applies is subdivided in Ranges II and III, depending on whether the velocity $\bar{c}$ of the inelastic front is larger or smaller than the velocity c_S of elastic shear waves, respectively. Range III, where $\bar{c} \leq c_S$, applies if

$$\sqrt{3}\alpha \leq -2+\frac{3}{\sqrt{[2(1+\nu)]}} \tag{95}$$

while Range II, $\bar{c} \geq c_S$, applies if equation (95) is violated. The reason for this division will be seen later.

3.1 *Range Ia*

As indicated above, the first step in the construction of solution is the determination of the range, designated Range Ia, in which entirely elastic solutions exist. In such a solution a P-wave enters a stressless region and an entirely elastic solution is possible, if at all, only in a range entirely within Range I, Fig. 9a. The stresses in an elastic half-space due to a superseismically traveling uniform surface pressure are given in Appendix A. There is a uniform state of stress between the P-front and S-front, and again a uniform, but different state of stress between the S-front and the surface, Fig. 10. The two uniform states of stress must satisfy the inequalities (69)

$$F \leq 0, \qquad J_1 \leq 0. \tag{96}$$

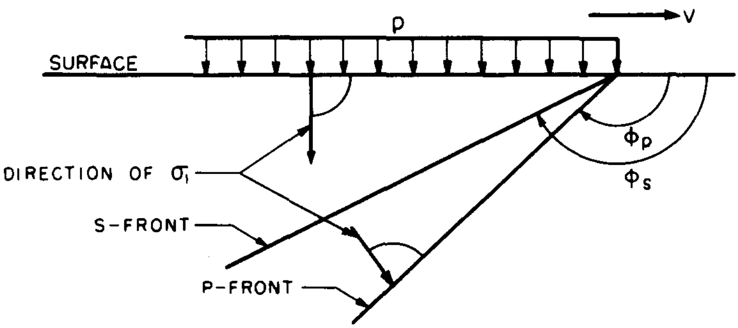

FIG. 10. Configuration for range Ia.

There is no need to check the validity of these inequalities in the region between the P and S fronts because this has actually been done in Section 2.3 where the existence of the P-front in Range I was proved. However, equations (96) must be considered for $\pi > \varphi > \varphi_S$. At the S-front a state of pure shear is added to the state of stress for $\varphi < \varphi_S$. This can not change the first invariant J_1 so that only the condition $F \leq 0$ requires checking.

Substitution of equations (138), (139) from Appendix A into this condition results in the inequality

$$\alpha^2 \geq \frac{1}{4}\left(\frac{1-2\nu}{1+\nu}\right)^2\left[\frac{\cos^2 2(\varphi_S-\varphi_P)}{\cos^2 2\varphi_S}+\frac{1}{3}\right] \tag{97}$$

where

$$\varphi_P = \pi - \sin^{-1}\left\{\frac{1}{V}\sqrt{\left[\frac{2G}{\rho}\frac{1-\nu}{1-2\nu}\right]}\right\} \tag{98}$$

$$\varphi_S = \pi - \sin^{-1}\left[\frac{1}{V}\sqrt{\left(\frac{G}{\rho}\right)}\right]. \tag{99}$$

The inequality (97) defines Range Ia where the response is entirely elastic. The range is a function of Poisson's ratio and of the value $V/c_P > 1$, and its boundary can be found by using the equal sign in equation (97). Figures 9b–d show that these boundaries end at the one between the principal Regions I and II, the endpoint being defined by the relation

$$\left[\frac{V}{c_p}\right]^2 = \frac{(1-2\nu)^2}{(1-\nu)(1-3\nu)}. \tag{100}$$

Figures 9b–d show Range Ia covering nearly all the Range I, while in Fig. 9e Range Ia actually covers all of Range I. It may be shown that for $V/c_p < 1{\cdot}061$ Range Ia covers all of Range I. The stresses in Range Ia are entirely elastic and are given by the simple relations listed in Appendix A.

3.2 *Range Ib*

It was found above that entirely elastic solutions exist only when the inequality (97) is satisfied. The remainder of Range I, i.e. the range

$$\frac{\sqrt{3}}{3} \leq \left(\frac{1+\nu}{1-2\nu}\right)\alpha < \frac{1}{2}\sqrt{\left[\frac{\cos^2 2(\varphi_S-\varphi_P)}{\cos^2 2\varphi_S}+\frac{1}{3}\right]} \tag{101}$$

will be designated as Range Ib. In this range the solution can no longer be entirely elastic and must therefore contain at least one location with inelastic deformation.

Using the expected continuity of the character of the solutions as a guide, the solution in this range ought to start again with a discontinuity which, according to Section 2.3, can only be an elastic P-front located at φ_P. Using equation (76) for the stress changes at the front, one finds that for* $\varphi = \varphi_P^{(+)}$ the inequality $F < 0$ is satisfied, provided the special case $\sqrt{3}\alpha = (1-2\nu)/(1+\nu)$ is excluded for separate consideration. Having recognized that the solution must contain an inelastic region, where $F = 0$, a further elastic stress change must occur, which is possible only at the S-front. The appropriate change in the state of stress at the S-front has been obtained in Appendix B, in terms of the as yet unknown stress discontinuity $\Delta\sigma$ at φ_P, as follows:

For $\varphi_P^{(+)} \leq \varphi \leq \varphi_S^{(-)}$:

$$\sigma_1 = \Delta\sigma, \qquad \beta = 3, \qquad \gamma = \frac{\pi}{2}, \qquad \theta = \varphi_P - \frac{\pi}{2} \tag{102}$$

* The symbol (+) in $\varphi_P^{(+)}$ indicates a value infinitesimally larger than φ_P.

while for $\varphi = \varphi_S^{(+)}$:

$$\beta = \sqrt{3}\left|\sqrt{\left[12\alpha^2\left(\frac{1+\nu}{1-2\nu}\right)^2 - 1\right]}\right| \tag{103}$$

$$J_1 = \frac{1+\nu}{1-\nu}\Delta\sigma \tag{104}$$

$$s_1 = \frac{(1-2\nu)(\beta+1)}{6(1-\nu)}\Delta\sigma \tag{105}$$

$$\gamma = \frac{\pi}{2} \mp |\delta| \tag{106}$$

$$\theta = \varphi_S - \frac{\pi}{2} \pm |\delta|. \tag{107}$$

The quantity δ is obtained from

$$\cos 2\delta = \frac{3}{\beta}\cos 2(\varphi_P - \varphi_S) \tag{108}$$

and is subject to the inequality

$$\varphi_S \geq |\delta| \geq \varphi_S - \varphi_P. \tag{109}$$

The special case $\sqrt{3}\alpha = (1-2\nu)/(1+\nu)$ remains to be discussed. In this case the yield condition $F = 0$ is satisfied already for $\phi = \phi_P^{(+)}$, so that the possibility of an inelastic region no longer requires a shear front at ϕ_S. However, a change in shear leading again to a state with $F = 0$ is still possible. For either possibility equations (103)–(108) apply. The special case simply means that one of the two values $\theta(\phi_S^{(+)})$ is equal to $\theta(\phi_P^{(+)})$ as given by equation (102).

The results obtained so far, and further steps required, are best discussed in terms of the angle θ in various locations, illustrated in Fig. 11. The direction of the principal stress between the P- and S-fronts according to equation (102) is normal to the P-front, while for $\varphi > \varphi_S^{(+)}$, equation (107) defines θ. Because of the inequality (109), $\theta(\varphi_S^{(+)})$ is less than

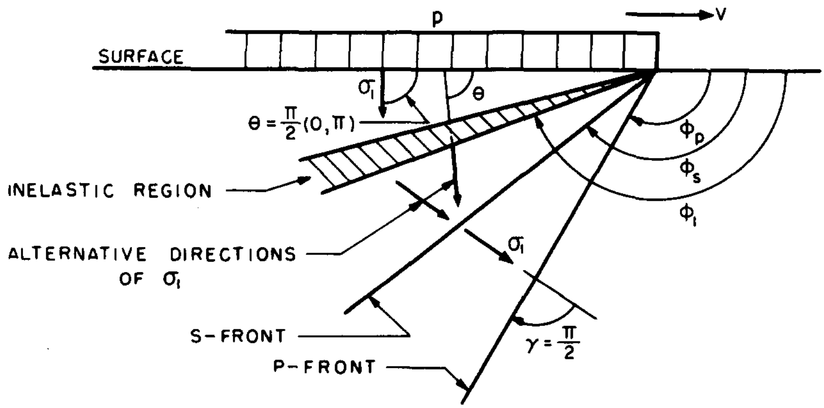

Fig. 11. Configuration for range Ib.

$\pi/2$ but more than 0, regardless of the sign of δ. According to Section 2, there is no further possibility for a change in θ as required to arrive at the surface value $\theta(\pi) = \pi/2$, (0 or π), except one or more inelastic regions for $\varphi > \varphi_S$.

Using the values of β, J_1, s_1, γ and θ defined by equations (103)–(107) the results of Section 2.1 are now to be used to find and determine the history of the stresses and particularly of the angle θ. If a region can be found during the forward integration where either of the values $\theta = \pi/2$ (or 0, or π) is obtained, the integration is terminated. From the point of termination to the surface an elastic region of no change is selected such that the surface condition for θ is then satisfied. During this integration the unknown value $\Delta\sigma$ in equations (104), (105) is a common factor in all stresses, so that the integration will give a principal stress at the surface which contains this factor. It is finally selected to satisfy the boundary condition, equation (91 or 92), $\sigma_{1,2} = -1$.

The use of the solutions derived in Section 2.1 for inelastic regions is quite straightforward. From the values of β, γ at $\varphi_S^{(+)}$, potential starting points φ_1 of inelastic regions are located as roots of the determinantal equation (30). Next it must be verified that GL/V, equation (39), is negative. If this is so, equations (34)–(37) are used to determine the solution by forward integration, continuously checking the sign of GL/V. The integration can be continued until GL/V changes sign, but may be stopped at any desired location φ_2. When an angle $\theta = \pi/2$ (or 0, or π) for the direction of the principal stress is obtained, a solution to the problem has been found.

The configuration was successful in all cases considered and led to just one solution of the problem. The upper sign in equation (107) and the case $\theta = \pi/2$ furnished the solution, but it is suspected that the other sign may apply when $V/c_P > 1$ is very close to unity. The matter of possible alternative configurations which might lead to solutions is discussed later in this section.

It is noted that Range Ib, which does not occur at all if $V/c_P < 1{\cdot}061$, applies even for other values of V/c_P only in a minute portion of the overall range of ν and α, as can be seen from Figs. 9(b–d).

3.3 *Range IIa*

According to the definition of ranges at the beginning of this section, an initial inelastic discontinuity, but no other, is possible in Range II. Further, in this range, the location $\bar{\varphi}$ of this discontinuity, defined by equation (66), is such that

$$\bar{\varphi} < \varphi_S. \tag{110}$$

Range II, which is the one of major interest, is defined by the combined inequalities (94, 95),

$$\frac{3}{\sqrt{[2(1+\nu)]}} - 2 < \sqrt{3}\,\alpha < \frac{1-2\nu}{1+\nu} \tag{111}$$

In that portion of Range II which adjoins Range Ia, Figs. 9(b–e), one expects that the solutions after starting with an inelastic front of discontinuity at $\bar{\varphi}$ will remain entirely elastic. The range in which such solutions apply and the values of the stresses are obtained in Appendix C. This range is designated Range IIa, and the stresses are found in closed form, the configuration being shown in Fig. 12.

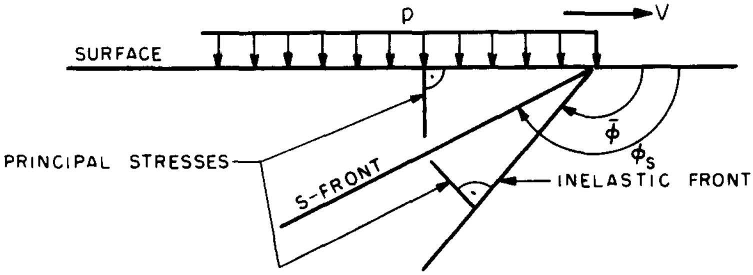

FIG. 12. Configuration for range IIa.

The discontinuity $\Delta\sigma$ in the normal stress at the front is

$$\Delta\sigma = \frac{-\cos 2\varphi_S}{(1-\bar{R})\cos^2(\bar{\varphi}-\varphi_S)+(1+\bar{R})\cos^2\varphi_S - 1} \tag{112}$$

where

$$\bar{R} = \frac{1-\alpha\sqrt{3}}{1+2\alpha\sqrt{3}}. \tag{113}$$

The principal stresses and their direction between the inelastic front and the shear front are

$\varphi_S^{(-)} \geq \varphi \geq \bar{\varphi}^{(+)}$:

$$\begin{aligned} \sigma_1 &= \Delta\sigma \\ \sigma_2 &= \sigma_3 = \bar{R}\Delta\sigma \\ \gamma &= \frac{\pi}{2}, \end{aligned} \tag{114}$$

while between the S-front and the surface

$\varphi \geq \varphi_S^{(+)}$:

$$\begin{aligned} \sigma_1 &= -1 \\ \sigma_2 &= -R, \qquad \sigma_3 = \bar{R}\Delta\sigma \\ \theta &= \frac{\pi}{2} \end{aligned} \tag{115}$$

where

$$R = -1-(1+\bar{R})\Delta\sigma \tag{116}$$

and σ_3 is the principal stress in the z direction.

The solution applies if the inequality

$$(1+2\alpha\sqrt{3})^2 - 36\alpha^2\cos^2\varphi_S \geq 6\left(\frac{1-2\nu}{1+\nu}\right)\cos^2\varphi_S \tag{117}$$

is satisfied. The boundary separating Region IIa from the remainder of Region II, designated Region IIb, is found by using the equal sign in the above relation. Figures 9(b–e) show typical curves for some values of V/c_P. These figures indicate that Range IIa covers only a quite small portion of Range II, except in the atypical case when V/c_P is only slightly larger than unity, Fig. 9e.

3.4 *Range IIb*

In Range II, but outside Range IIa, the solutions are expected to start with an inelastic pressure front at $\bar{\varphi}$, but additional inelastic regions must now occur. In the vicinity of the boundary towards Region Ib, continuity requires similar configurations, as shown in Fig. 13. Behind the inelastic front the stresses will be uniform with a shear front at φ_S, and a region of inelastic deformation in a location $\varphi_S < \varphi < \pi$. The discontinuity in shear $\Delta\tau$ must be such that the yield condition $F = 0$ is satisfied for $\varphi \geq \varphi_S^{(+)}$.

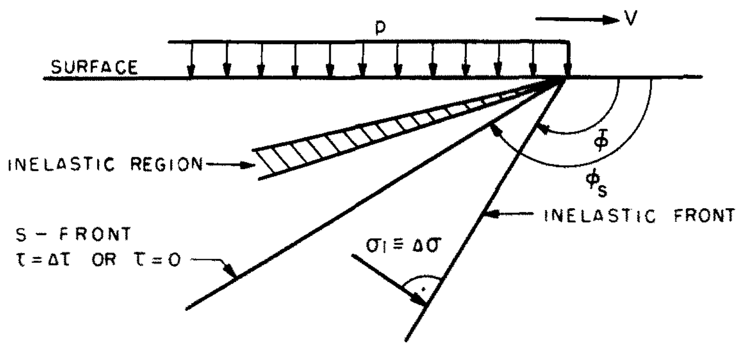

Fig. 13. Configuration for range IIb.

However, at points remote from the boundary between Regions Ib and IIb alternative configurations might occur and must be considered as possibilities in the numerical analysis. In the configuration shown in Fig. 13 the possibility $\Delta\tau = 0$ could furnish a solution, or inelastic regions may exist in locations $\bar{\varphi} < \varphi < \varphi_S^{(-)}$, as shown in the alternative Figs. 14 and 15, where shear discontinuities $\Delta\tau \neq 0$, may occur, or not, $\Delta\tau = 0$.

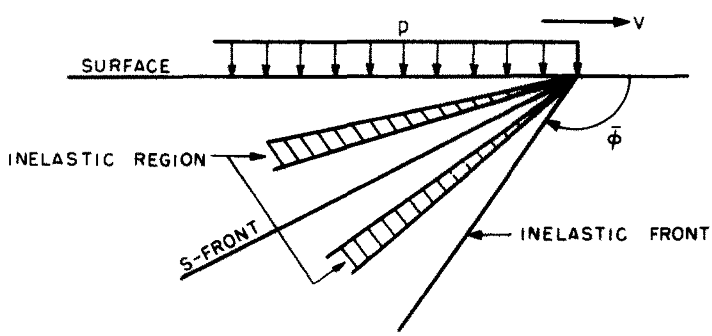

Fig. 14. Alternative configuration.

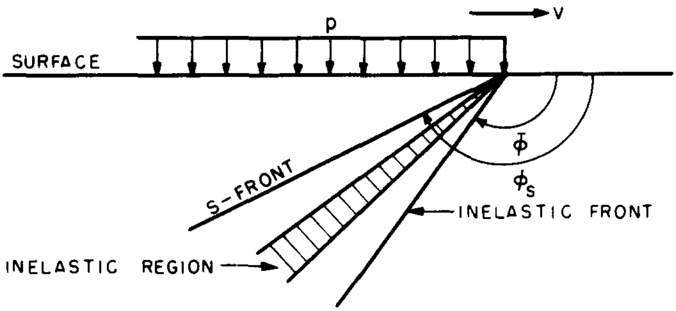

FIG. 15. Alternative configuration.

Further, the configuration shown in Fig. 15 may have a subrange where the discontinuity $\Delta\tau$ is such that elastic conditions $F < 0$ are created and, therefore, constant stresses occur for $\varphi > \varphi_S^{(+)}$. Disregarding, for later discussion, solutions without initial discontinuity, but allowing inelastic regions to split, this exhausts all possibilities to be studied. In all cases considered the numerical analysis by computer furnished only solutions having the configuration of Fig. 13. The search for roots of the determinantal equation, giving starting points of inelastic regions never furnished a root for $\phi < \phi_S$.

The following statement summarizes the situation. The initial change from vanishing to nonvanishing stresses occurs at an inelastic front with an as yet undetermined compressive discontinuity $\Delta\sigma$ in the principal stress σ_1. This front is followed by a region of constant stress, for $\varphi_S^{(-)} > \varphi > \bar{\varphi}^{(+)}$:

$$\begin{aligned} \sigma_1 &= \Delta\sigma \\ \beta &= 3 \\ \theta &= \frac{\pi}{2} . \end{aligned} \tag{118}$$

For locations $\varphi > \varphi_S$ there are two alternatives. If no discontinuity in shear occurs, $\Delta\tau = 0$, equations (118) apply also for $\varphi = \varphi_S^{(+)}$, while the angle γ is

$$\gamma(\varphi_S^{(+)}) = \varphi_S - \bar{\varphi} + \frac{\pi}{2} . \tag{119}$$

However, if a shear discontinuity, $\Delta\tau \neq 0$, occurs, equations (86), (87) give, using $\bar{\gamma} = \varphi_S - \varphi + \pi/2$,

for $\varphi_S^{(+)}$:

$$\begin{aligned} \sigma_1 &= \Delta\sigma \\ \beta &= 3 \\ \gamma &= \frac{\pi}{2} \\ \theta &= 2\varphi_S - \bar{\varphi} - \frac{\pi}{2} . \end{aligned} \tag{120}$$

Equations (120) and the alternative values for $\Delta\tau = 0$ are the starting points for numerical integrations which are to be carried out in the manner described for Range Ib.

3.5 *Search for inelastic solutions without initial discontinuity*

In Ranges I and II solutions were constructed where the initial change, from vanishing to nonvanishing stresses, occurred as a shock, either elastic at φ_P, or inelastic at $\bar{\varphi}$. While the principle of the continuity of solutions makes the solutions obtained plausible, it is necessary to investigate if solutions which start smoothly exist.

The differential equations in elastic regions permit definitely no smooth change in stress for superseismic velocities V, so that only the inelastic case is considered.

If a smooth inelastic solution starting from vanishing stresses in a location φ_0 exists, an asymptotic study of the appropriate differential equations for $\sigma_j = s_j = J_1 \to 0$ in the vicinity of φ_0 must describe this solution. In order to be physically sensible, the angle γ in the vicinity of φ_0 must be well behaved and may be considered a constant in the range $\varphi_0 \leq \varphi \leq \varphi_0 + \varepsilon$ where ε is small. The quantity $GL/V < 0$ must not vanish, otherwise the region is not inelastic as postulated. There are, however, two possibilities for the behavior of GL/V. In the limit $\varphi \to \varphi_0$, the function GL/V may be finite and well behaved, in which case it may be considered a constant near φ_0; alternatively, GL/V may, in the limit, be infinite.

The first possibility, where GL/V in the limit may be replaced by a constant is easily proved to be impossible. Following the previous reasoning in Section II, solutions in an inelastic region exist only if the determinant of equations (25) vanishes, in which case four of the five unknowns will depend on the fifth. In the limit s_j, $J_1 \to 0$ the last equation (25) becomes trivial, $0 \equiv 0$. The last terms of the other equations vanish, because GL/V is finite and products of GL/V and s_j or J_1 in the limit are therefore zero. The remaining four equations are then identical with the four equations (70) in the elastic case. They have nonvanishing solutions only when $\varphi_0 = \varphi_S$ or $\varphi_0 = \varphi_P$. However, the yield condition, $F = 0$, represented by the last equation (25), which became trivial, may now not be satisfied and must be checked. In the vicinity of s_j, $J_1 \to 0$, the ratio of these stresses must obviously be the same as at the P- or S-front, equations (76) and (80), respectively, obtained from the same equations. Based on the discussion of the P- and S-fronts, one finds easily that the requirement $F = 0$ is not satisfied, except in the special case when the values α and ν are exactly on the boundary between regions I and II, where $\bar{\varphi} \equiv \varphi_P$. However, in this case one finds $GL/V \equiv 0$, and no inelastic solutions whatsoever are therefore possible when GL/V at φ_0 is finite.

The case where $|GL/V| \to \infty$ as $\varphi \to \varphi_0$ remains to be discussed. The first question concerns the possibility of $|GL/V| \to \infty$ and conditions for the occurrence of such a singularity. If such a point exists for some values of γ and of the ratios of s_j and J_1, when the latter are small, $\to 0$, then $|GL/V| \to \infty$ would also occur for the same ratios if s_j and J_1 are finite. Equations (34), (35) and (37) which apply, would then give infinite values for one or more of the derivatives s'_j, J'_1. The possibility $|GL/V| \to \infty$ exists therefore only in locations where an inelastic front of discontinuity may occur and the conditions required are those for such a front. Using the results of Section 2.2 for inelastic discontinuities, no smooth solution can exist in Region I, because no inelastic shock front is possible. In Regions II and III where such a front may occur at $\bar{\phi}$, a solution of the type sought may exist, starting at $\phi_0 = \bar{\phi}$; the necessary initial values of the state of stress being again defined by

$$\beta(\varphi_0) = 3$$
$$\gamma(\varphi_0) = \frac{\pi}{2}. \quad (121)$$

If such an inelastic solution in a region $\phi \geq \bar{\phi}$ of finite extent actually exists, the determinantal equation (30) must be satisfied for $\phi > \bar{\phi}$. This is necessary because the previous reasoning only implies that this equation is satisfied for $\phi = \bar{\phi}$. To explore this point an asymptotic expression for equation (30) is obtained by substituting

$$\varphi = \bar{\varphi} + \varepsilon$$
$$\beta = 3 + \Delta \quad (122)$$
$$\gamma = \frac{\pi}{2} + \eta$$

where ε, Δ and η are small quantities. Retaining the lowest order terms in the new variables one obtains the determinantal equation in the asymptotic form

$$b_8\eta^2 - \Delta^2 = b_9\varepsilon \quad (123)$$

where the quantities b_8 and b_9 are functions of ν, α and V/c_P, given in Appendix D. The quantity b_9 is always positive, while b_8 may be positive or negative, changing the character of the equation radically.

In Range II, i.e. when the inequality (111) applies, b_8 is negative so that the equation has real roots only for negative ε. While an inelastic region can exist for $\varphi < \bar{\varphi}$ ending at $\bar{\varphi}$ with vanishing stresses, no such regions can exist for $\varphi > \bar{\varphi}$, i.e. in the location of interest here. The solutions in Ranges I and II with an initial discontinuity previously considered are the only ones possible.

In Range III, where the inequality (95) applies, one finds $b_8 > 0$, so that the determinantal equation (123) has real roots for $\varepsilon > 0$ as necessary for solutions without initial discontinuity in stress. The final condition, $GL/V < 0$, is also satisfied, because the stress ratios in this region are initially equal to those for the inelastic front, where $GL/V < 0$. All requirements are therefore satisfied and it is concluded that in Range III, and only in this range, an inelastic solution without stress discontinuity exists. The details of its determination are given in Appendix D.

3.6 *Range III*

According to the definition of ranges, an inelastic shock front in the location $\bar{\varphi}$ is possible, and one can attempt to construct a solution starting with this discontinuity in analogy to Range II. However, the computational search for inelastic regions, for $\varphi > \bar{\varphi}$, was unsuccessful, and the boundary conditions on the surface can not be satisfied without such an inelastic region. While the determinantal equation (30) is nonlinear and too complex to prove the nonexistence of roots in general, the approximate equation (123) furnishes a partial proof, as there is obviously no root $\Delta = \eta = 0$ for $\varepsilon > 0$.

The impossibility of finding a solution with an initial discontinuity is, however, very satisfactory because the previous subsection and Appendix D indicate that in this range a solution exists which starts at $\varphi = \bar{\varphi}$ without discontinuity. Because of their singular character the differential equations at and near the starting point can not be solved by the numerical procedure used in the other ranges. Therefore, the asymptotic solution obtained in Appendix D must be applied for a small range $\varphi \geq \bar{\varphi}$, until the solutions are sufficiently well behaved to return to the numerical integration of the differential equations obtained in Section IIa.

To start the solution, equation (175) gives $\Delta \sim 0$ so that in the proximity of $\phi = \bar{\phi}$ the value of β becomes approximately

$$\beta = 3+\Delta \sim 3 \tag{124}$$

while

$$\gamma = \frac{\pi}{2}+\eta \tag{125}$$

where the small quantity $|\eta|$ is inherently larger than the neglected value $|\Delta|$. Equation (176), and a similar expression for the principal stress σ_1, contains an arbitrary constant C_0. If $\varphi_e = \bar{\varphi}+\varepsilon_e$ is the end point of the asymptotic region, the value of the principal stress $\sigma_1(\varphi_e)$ may be used as the arbitrary constant instead of C_0. Choosing a value $\eta = \eta_e$, small, yet large enough for the numerical integrations to work thereafter, one searches for the corresponding value φ_e where the determinantal equation is satisfied by the combination of $\beta = 3$, $\gamma_e = \eta_e+\pi/2$ and φ_e. The principal stress $\sigma_1(\varphi_e)$ at this point can be made equal to unity. From this point on integration proceeds exactly as in the other ranges. Due to the fact that equation (174) defining η has a $\pm$ sign, it is necessary to include the two possibilities $\pm\eta_0$.

The procedure outlined was found to be successful, one, and only one, of the integrations for $\pm\eta_e$ furnishing a solution. The stresses in the interval $\bar{\varphi}$ to φ_e increase as $(\varphi-\bar{\varphi})^n$. To obtain their distribution the exponent n can be obtained from equation (177). n is a very small positive number, of the order of 1/100. The configuration of solutions in Range III is shown in Fig. 16.

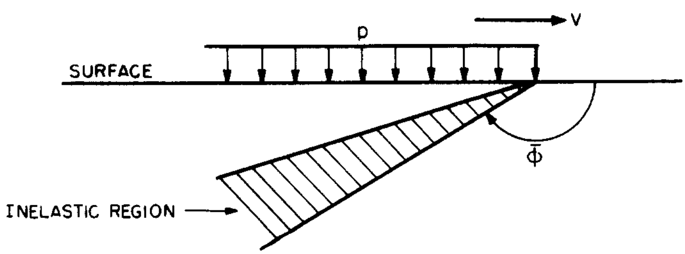

FIG. 16. Configuration for range III.

The occurrence of solutions with and without initial discontinuity in stress, does not break the continuity in the character of the solutions. Even for the continuous solutions the derivative of the stresses at $\bar{\varphi}$ is infinite, as at a discontinuous front, and the numerical results indicate that the change in stress in the asymptotic region due to the small exponent n is so rapid, that this region is practically indistinguishable from a discontinuity, see Fig. 17.

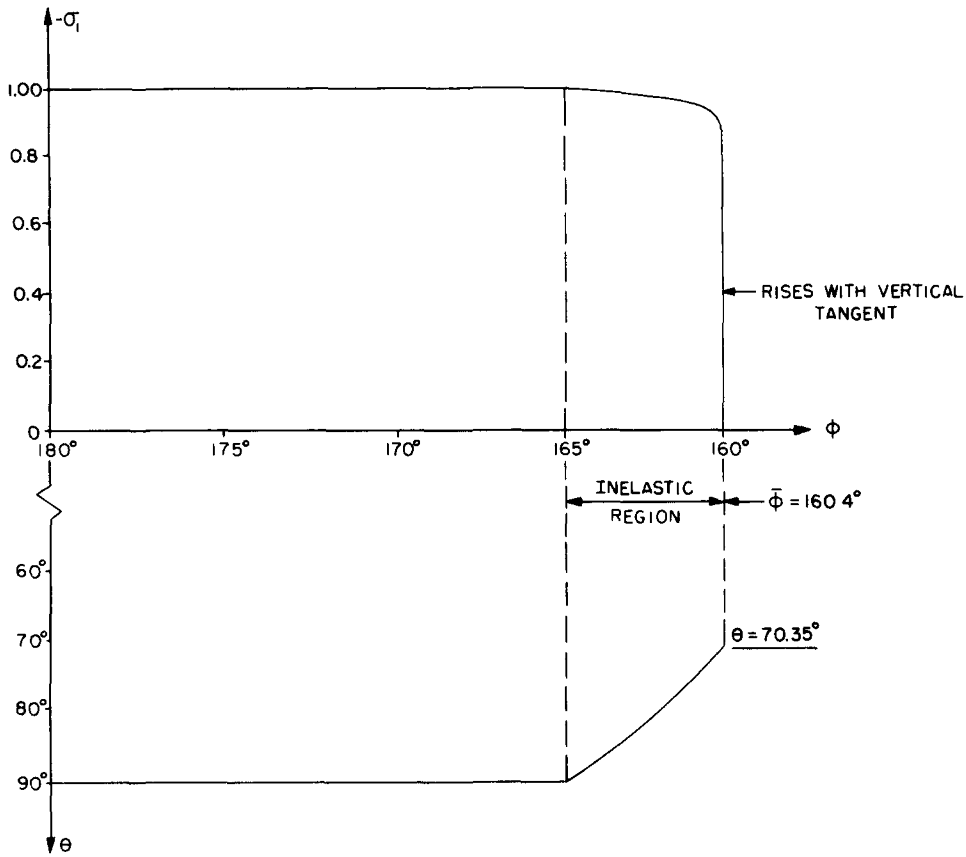

FIG. 17. Typical result in range III ($\nu = 0$, $\alpha = 0{\cdot}05$, $V/c_P = 2$).

3.7 *Numerical analysis*

In Ranges Ib, IIb and III a numerical search for inelastic regions, and subsequent numerical quadratures are required. In Section 2 the basic equations have been written in a very abbreviated form, somewhat concealing the complexity of these relations. The solution of these equations by hand computation is impractical, and the computations were made on an IBM 7094. A common program was devised, allowing for the different configurations which may occur.

The inelastic regions are always quite narrow as functions of φ, only a few degrees, and become even narrower as V/c_P becomes large. It was therefore necessary to vary the intervals of φ in the search and in the quadratures. For $V/c_p \leq 2$ intervals of 1/500 rad were used, while for $V/c_p = 5$ intervals of 1/10,000 rad were selected.

The results obtained are discussed in Section 4.

4. NUMERICAL RESULTS AND CONCLUSION

4.1 *Results*

The effects of a step pressure progressing with superseismic velocity $V > c_p$ on a half-space have been obtained for an elastic–plastic medium subject to the yield condition

(4), representing an inelastic material governed by internal Coulomb friction. The solutions depend on the elastic material parameters E and ν, and on the additional parameter $\alpha < \sqrt{(1/12)}$ in equation (4). α is related to the angle Φ of internal friction, using equation (10) of Ref. [6],

$$\sin \Phi = \frac{3\alpha}{\sqrt{(1-3\alpha^2)}}. \tag{126}$$

In spite of the lack of a general uniqueness and existence theorem, one, and only one solution was obtained for each combination of material parameters, surface load p, and velocity $V/c_P > 1$ which was considered. One finds, however, radically different configurations, depending on the values of the nondimensional parameters ν, α and V/c_P. The ranges in which the various configurations apply have been designated by I, II and III, where Ranges I and II have been subdivided into Subranges a and b. The values of the parameters ν and α alone determine which of the Ranges I, II or III applies in a particular case, as shown in Fig. 9a, while the subdivision into a or b depends on the value of V/c_P, typical cases being shown in Figs. 9b–e. These figures show that Ranges Ia and IIb cover most of the total range in ν and α, the other ranges being of very limited applicability.

Range Ia gives entirely elastic solutions, known from Ref. [1], and is not further considered.

The parameter α is inherently restricted, $\alpha \leq 1/\sqrt{12}$, but sensible values for the angle Φ of internal friction, equation (126), permit a further limitation to the range $0{\cdot}10 \leq \alpha \leq 0{\cdot}20$. Numerical results were therefore obtained, as indicated in Figs. 9b–d, for combinations of $V/c_P = 1{\cdot}25$, 2, 5, $\nu = 0$, 1/8, 1/4, 1/3, and $\alpha = 0{\cdot}10$, $0{\cdot}15$, $0{\cdot}20$. The values α selected cover the range $\sin \Phi = 0{\cdot}3$–$0{\cdot}7$. Except for two points which fall in Range IIa, all these combinations are in Range IIb. For completeness the result for one case in Range III, $\nu = 0$, $\alpha = 0{\cdot}05$, $V/c_P = 2$ was also obtained.

Figure 18 shows a typical variation of the principal stress σ_1 and of the angle θ in the major Range IIb. There is a discontinuous rise in the principal stress σ_1 at the inelastic front, followed by a discontinuity in direction θ, but not in magnitude of σ_1, at the S-front. There is further a minor increase in σ_1 in the inelastic region combined with a change in direction, θ. For unit step pressures, $p_0 = 1$, Table 1 gives the values of the principal stresses σ_1, σ_2, σ_3, and of the angle θ, and the locations of the fronts for all cases considered, which fall into Range IIb.

Figures 19a, b show σ_1 and θ for the two cases, $\nu = 1/3$, $\alpha = 0{\cdot}10$, $V/c_P = 1{\cdot}25$ and $2{\cdot}0$, which fall into Range IIa. In these cases the initial stress rise is again at the inelastic front, $\varphi = \bar{\varphi}$. There is a change in σ_1 and θ at the S-front, but there are no further inelastic regions, and no further changes in σ_1 or θ. The solution in this range does not require numerical integrations, but is entirely in closed form.

Range III is only of limited interest, because it applies only for very low angles Φ, $\sin \Phi < 0{\cdot}21$, but a typical case is shown in Fig. 17. There is no discontinuous front, the solution starts smoothly at $\phi = \bar{\phi}$, but the principal stress σ_1 has a vertical tangent and rises extremely rapidly, and the situation is practically the same as at a discontinuous front.

4.2 *Effect of cohesion*, $k \neq 0$

If the more general equation (1) for the plastic potential is used, instead of equation (4), the differential equations for inelastic regions and their solutions derived in Section 2.1 remain valid. However, the configurations of the complete solutions found in Section 3 change, because of the different yield condition. The nature of these changes can be

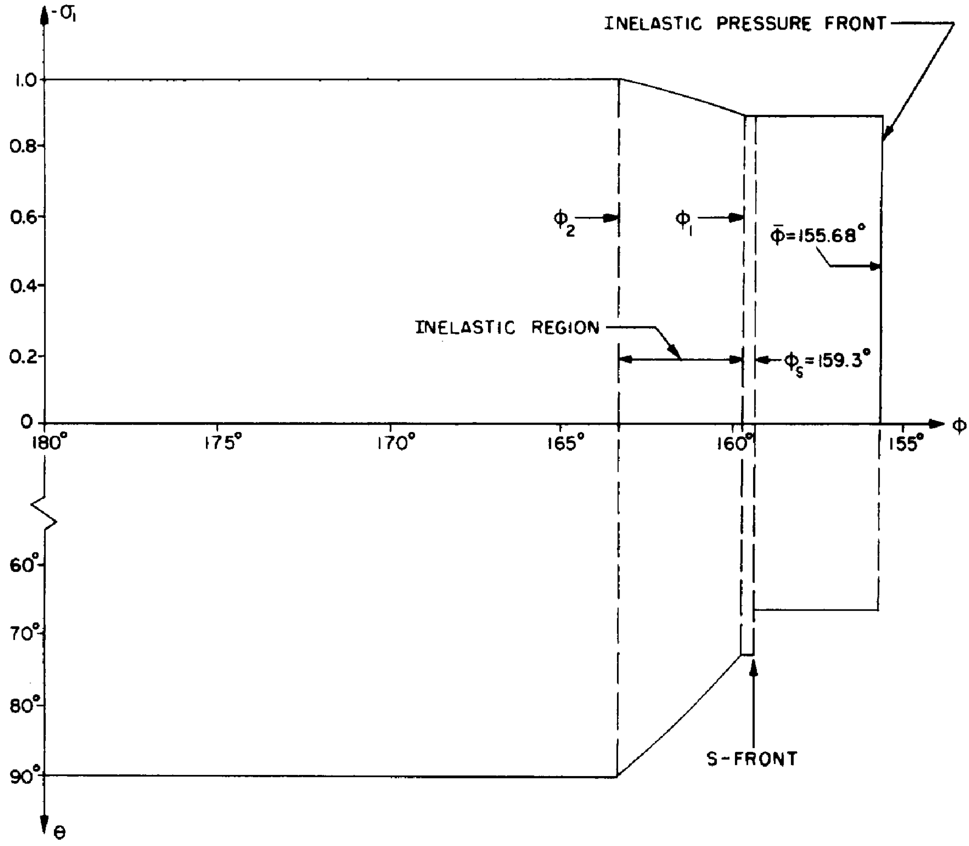

FIG. 18. Typical result in range IIb ($\nu = 0, \alpha = 0{\cdot}15, V/c_p = 2$).

predicted from the available solution [5] for a von Mises elasto–plastic material, for which equation (1) applies with $k \neq 0$, but $\alpha = 0$. The most general configuration for the latter material is according to Fig. 20. The solution always begins with an elastic P-front, has an S-front, and may have two (or less) inelastic regions of finite thickness as shown. No plastic shock ever occurs. The arguments used in [5] to obtain the configuration shown in Fig. 20, hold equally for the more general case when the plastic potential (1) applies, and one can predict therefore that the solutions for the latter case must have configurations covered by Fig. 20.

The transition from the configuration shown in Fig. 20 to those found in the present paper requires consideration of a limiting process. The general solution for $k \neq 0$, is a function of the ratio p_0/k. In the present solution it was assumed $p_0 = 1$, $k \to 0$, so that $p_0/k \to \infty$. Consider as a typical example the situation for Range IIb where the configuration, Fig. 13, must follow from the one in Fig. 20 when $p_0/k \to \infty$. In the configuration according to Fig. 20 the stresses between the P-front and the first plastic zone must be of the order k, i.e. the stresses are quite small compared to the surface load. To reach the large surface value p_0/k, large changes in the stresses must occur somewhere in the range, $\phi_p < \phi < \pi$. This can happen only in one of the plastic regions. For large values of p_0/k

TABLE 1. RESULTS IN RANGE IIb

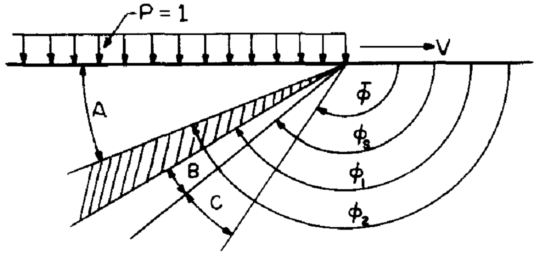

							Location					
							A†		B	B and C		C
V/c_P	ν	φ_S^*	α	$\bar{\varphi}^*$	φ_1^*	φ_2^*	$-\sigma_2$	$-\sigma_3$	θ^*	$-\sigma_1$	$-\sigma_2$ $-\sigma_3$	θ^*
			0·10	142·84	146·05	157·90	0·5788	0·6586	58·26	0·8111	0·4981	52·80
	0	145·55	0·15	138·79	146·73	156·55	0·4352	0·5523	62·31	0·7950	0·3872	48·79
			0·20	135·40	147·21	155·40	0·3202	0·4677	65·70	0·7881	0·3043	45·40
			0·10	137·51	150·41	157·71	0·5804	0·6560	69·32	0·8987	0·5519	47·51
1·25	1/8	148·42	0·15	133·47	150·96	156·51	0·4424	0·5411	73·37	0·8791	0·4282	43·47
			0·20	130·52	151·21	155·50	0·3346	0·4467	76·32	0·8794	0·3395	40·52
			0·10	131·53	156·15	158·26	0·5973	0·6326	83·46	0·9641	0·5920	41·53
	1/4	152·49	0·15	128·42	156·27	157·29	0·4733	0·5016	86·57	0·9743	0·4746	38·42
			0·20	127·06	156·01	156·58	0·3753	0·3972	87·92	0·9813	0·3789	37·06
			0·10	157·82	159·41	164·01	0·5960	0·6342	70·77	0·8954	0·5498	67·82
	0	159·30	0·15	155·68	159·55	163·17	0·4615	0·5155	72·91	0·8943	0·4356	65·68
			0·20	153·97	159·64	162·53	0·3547	0·4206	74·62	0·8955	0·3457	63·97
			0·10	155·03	161·35	164·03	0·5979	0·6319	76·76	0·9441	0·5797	65·03
2·0	1/8	160·89	0·15	153·03	161·44	163·43	0·4662	0·5098	78·76	0·9410	0·4584	63·03
			0·20	151·63	161·47	162·99	0·3622	0·4118	80·16	0·9409	0·3633	61·63
			0·10	152·10	164·06	164·97	0·6053	0·6233	84·34	0·9791	0·6012	62·10
	1/4	163·22	0·15	150·68	164·04	164·62	0·4776	0·4969	85·76	0·9799	0·4773	60·68
			0·20	150·08	163·95	164·38	0·3760	0·3965	86·36	0·9801	0·3784	60·08
			0·10	171·31	171·88	172·54	0·6105	0·6177	82·43	0·9703	0·5958	81·31
	0	171·87	0·15	170·52	171·89	172·30	0·4823	0·4920	83·22	0·9761	0·4754	80·52
			0·20	169·89	171·89	172·18	0·3805	0·3918	83·85	0·9789	0·3779	79·89
			0·10	170·28	172·51	172·78	0·6111	0·6171	84·67	0·9887	0·6071	80·28
5·0	1/8	172·48	0·15	169·55	172·51	172·69	0·4834	0·4908	85·41	0·9889	0·4817	79·55
			0·20	169·04	172·51	172·64	0·3820	0·3903	85·91	0·9893	0·3820	79·04
			0·10	169·21	173·42	173·50	0·6125	0·6156	87·53	0·9960	0·6116	79·21
	1/4	173·37	0·15	168·70	173·42	173·47	0·4854	0·4888	88·03	0·9961	0·4852	78·70
			0·20	168·49	173·41	173·45	0·3842	0·3879	88·25	0·9961	0·3846	78·49
	1/3	174·26	0·10	168·61	174·33	174·33	0·6140	0·6141	89·91	0·9999	0·6140	78·61

* In degrees.
† In this location $\sigma_1 = -1$, $\theta = 90°$.

extremely rapid and large stress changes were found, [5], for the von Mises material near the location $\bar{\phi}$, which corresponds to the location of the inelastic shock front in Fig. 13. This indicates that the configuration of the latter figure is a limiting case of that in Fig. 20, in which the stresses ahead of the first plastic region go towards zero in the same manner as k, while the plastic region near $\bar{\phi}$ degenerates into an infinitely narrow region, i.e. into a plastic front. The situation in other ranges can be explained similarly.

It is interesting to note that the numerical solution for the von Mises material encountered numerical difficulties if $p_0/k \gg 1$, because stress gradients near $\phi = \bar{\phi}$ become extremely large. To overcome these difficulties asymptotic solutions near $\phi = \bar{\phi}$ were obtained in [5]. The solution obtained in the present paper for the Coulomb material for $k \to 0$ are the corresponding, but much more complex asymptotic solutions for $p_0 \gg k$ for a material with the plastic potential (1).

There is no difficulty in obtaining the numerical solution for $\alpha \neq 0$, $k \neq 0$ from the relations derived in the paper using the configuration developed in [5]. However, due to the dependency on three parameters a tabulation of the results would become quite lengthy.

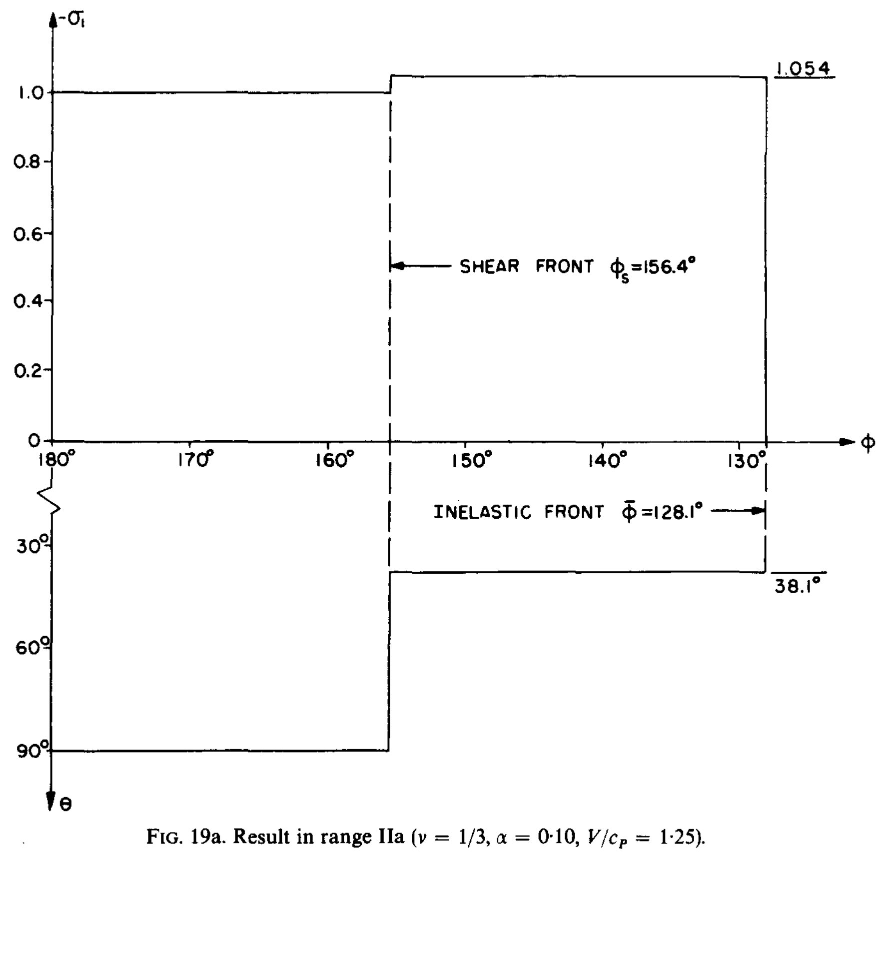

FIG. 19a. Result in range IIa ($\nu = 1/3$, $\alpha = 0{\cdot}10$, $V/c_P = 1{\cdot}25$).

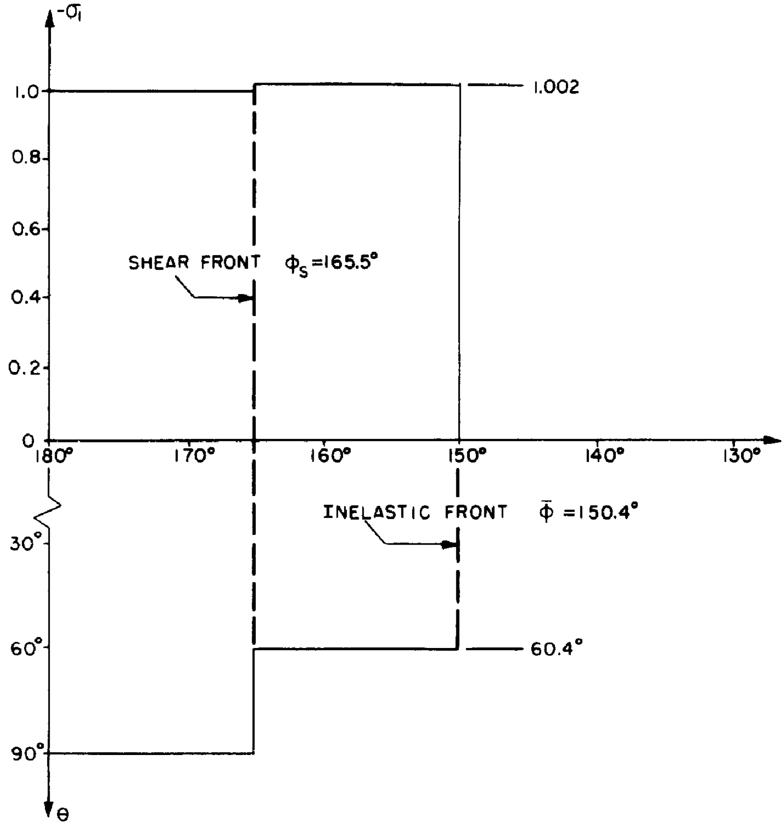

FIG. 19b. Result in range IIa ($\nu = 1/3$, $\alpha = 0{\cdot}10$, $V/c_P = 2{\cdot}0$).

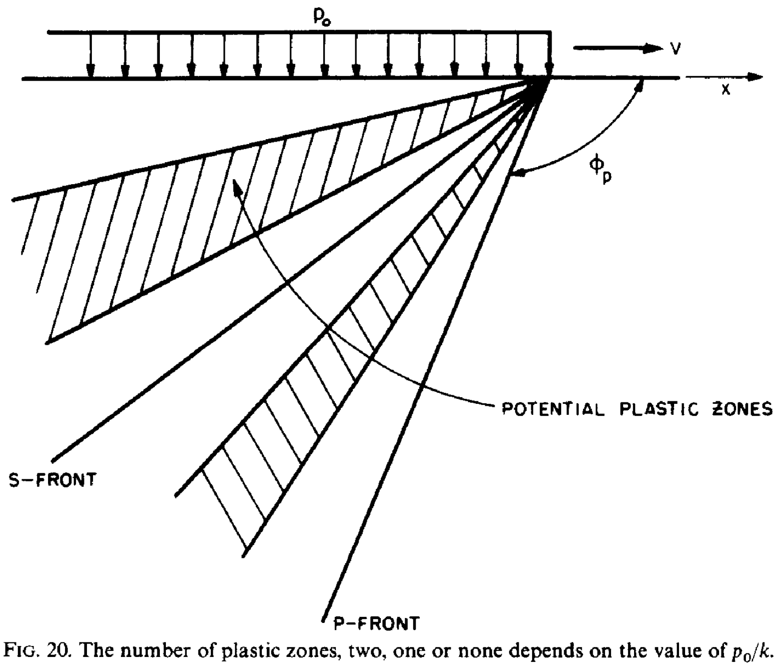

FIG. 20. The number of plastic zones, two, one or none depends on the value of p_0/k.

REFERENCES

[1] J. D. COLE and J. H. HUTH, Stresses produced in a half-plane by moving loads. *J. appl. Mech.* **25**, 433–436 (1958).
[2] J. W. MILES, On the response of an elastic half-space to a moving blast wave. *J. appl. Mech.* **27**, 710–716 (1960).
[3] J. L. SACKMAN, Uniformly progressing surface pressure on a viscoelastic half-plane. *Proc. 4th U.S. Natn. Congr. appl. Mech.*, June 1962.
[4] J. W. WORKMAN and H. H. BLEICH, The effect of a moving load in a viscoelastic half-space. Office of Naval Research, Tech. Rpt 12, Contract Nonr 266(34), November (1962).
[5] H. H. BLEICH and A. T. MATTHEWS, Step load moving with superseismic velocity on the surface of an elastic–plastic half-space. *Int. J. Solids Struct.* **3**, 819–852 (1967).
[6] D. C. DRUCKER and W. PRAGER, Soil mechanics and plastic analysis or limit design. *Q. appl. Math.*, p. 157 (1952).
[7] H. H. BLEICH and I. NELSON, Plane waves in an elastic–plastic half-space due to combined surface pressure and shear. *J. appl. Mech.* **33**, 149–158 (1966).
[8] H. H. BLEICH, A. T. MATTHEWS and J. W. WRIGHT, Step load moving with superseismic velocity on the surface of a half-space of granular material. Air Force Weapons Laboratory, Tech. Rpt No. AFWL-TR-65-59, September (1965).
[9] J. MANDEL, Ondes plastiques dans un milieu indéfini à trois dimensions. *Jnl Méc.* **1**, 3–30 (1962).

APPENDIX A

STEADY-STATE SOLUTION FOR AN ELASTIC HALF-SPACE

As background for Section 3, the details of the solution of the steady-state problem for an elastic half-space are derived. The values of the stresses in Cartesian coordinates could be obtained by integration from Ref. [1] and the desired principal stresses could be computed. However, it is just as easy to obtain the latter directly from the knowledge of the location of the shock fronts φ_P and φ_S in Fig. A1, coupled with the necessity of uniform stresses for $\varphi_S > \varphi > \varphi_P$ and $\pi > \varphi > \varphi_S$. The values φ_P and φ_S depend on the velocities of the fronts given by equation (98) and (99).

Designating the principal stresses in the region $\varphi_S > \varphi \geq \varphi_P$ by $\bar{\sigma}_1$, $\bar{\sigma}_2$ and $\bar{\sigma}_3 \equiv \sigma_z$ it follows from equation (76) that

$$\bar{\sigma}_1 = \Delta\sigma \qquad \bar{\sigma}_2 = \bar{\sigma}_3 = \frac{\nu}{1-\nu}\Delta\sigma \tag{127}$$

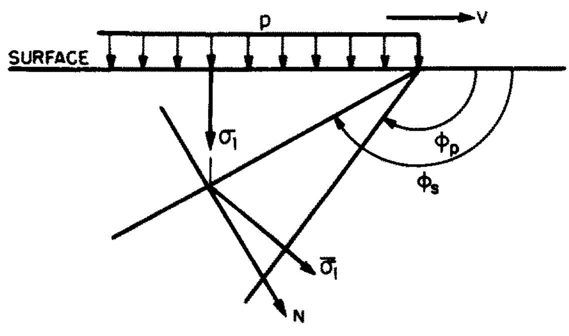

FIG. A1

where the jump $\Delta\sigma$ remains to be determined. The direction of $\bar{\sigma}_1$ makes an angle $(\varphi_S - \varphi_P)$ with the normal N to the S-front. The normal stress σ_N, and the tangential stress σ_T with respect to the S-front in the x–y plane can be expressed by the principal stresses $\bar{\sigma}_1$ and $\bar{\sigma}_2$,

$$\sigma_N = \Delta\sigma\left[\cos^2(\varphi_S - \varphi_P) + \frac{\nu}{1-\nu}\sin^2(\varphi_S - \varphi_P)\right] \tag{128}$$

$$\sigma_T = \Delta\sigma\left[\sin^2(\varphi_S - \varphi_P) + \frac{\nu}{1-\nu}\cos^2(\varphi_S - \varphi_P)\right]. \tag{129}$$

In the region $\pi \geq \varphi > \varphi_S$ the principal stresses are σ_1, σ_2 and $\sigma_3 \equiv \sigma_z$. The surface condition requires that $\sigma_1 = -1$ be vertical, making an angle $(\pi - \varphi_S)$ with the normal to the shear front. The normal and tangential stresses (with respect to the S-front) are therefore

$$\sigma_N = -[\cos^2\varphi_S + R\sin^2\varphi_S] \tag{130}$$

$$\sigma_T = -[\sin^2\varphi_S + R\cos^2\varphi_S] \tag{131}$$

where

$$R \equiv \frac{\sigma_2}{\sigma_1} = -\sigma_2. \tag{132}$$

There being no discontinuity in the normal and tangential stresses at a shear front, σ_N and σ_T in equations (128)–(131) can be equated and give two simultaneous equations for $\Delta\sigma$ and R. The stresses σ_3 and $\bar{\sigma}_3$ in the z direction must also be equal, $\sigma_3 = \bar{\sigma}_3$. Using the abbreviation

$$N = \cos^2\varphi_S + (1-2\nu)\cos^2(\varphi_S - \varphi_P) - 1 + \nu \tag{133}$$

the discontinuity at the P-front for a unit surface load becomes

$$\Delta\sigma = -\frac{(1-\nu)}{N}\cos 2\varphi_S. \tag{134}$$

In the region $\varphi > \varphi_S$ the principal stresses are

$$\sigma_1 = -1 \tag{135}$$

$$\sigma_2 = 1 - \frac{\cos 2\varphi_S}{N} \tag{136}$$

$$\sigma_3 = -\frac{\nu}{N}\cos 2\varphi_S \tag{137}$$

while the invariants become

$$J_1 = -\frac{(1+\nu)}{N}\cos 2\varphi_S \tag{138}$$

$$J_2 = 1 - \frac{\cos 2\varphi_S}{N} + \frac{(1-\nu+\nu^2)}{3N^2}\cos^2 2\varphi_S. \tag{139}$$

It is noted that φ_P and φ_S are functions of ν in such fashion that N for $V/c_P > 1$ is necessarily positive, so that the condition $J_1 < 0$ is always satisfied. However, the yield inequality gives a condition on α, equation (78) in the text.

APPENDIX B

ANALYSIS FOR RANGE Ib

In this range discontinuous elastic stress changes occur at the P- and S-fronts so that the combined effect satisfies the yield condition at $\varphi = \varphi_S^{(+)}$. The following derives the required details of the state of stress for $\varphi \geq \varphi_S^{(+)}$.

Using an approach similar to that in Appendix A, the stresses in the region $\varphi_S^{(-)} \geq \varphi > \varphi_P^{(+)}$ are given by equations (127), and the normal and tangential stresses with respect to the S-front by equations (128), (129). The principal stress σ_1 for $\varphi = \varphi_S^{(+)}$ will, in this range, make an unknown angle δ with the normal N to the S-front, Fig. A2, and σ_N and σ_T become alternatively

$$\sigma_N = \sigma_1 \cos^2 \delta + \sigma_2 \sin^2 \delta \tag{140}$$

$$\sigma_T = \sigma_1 \sin^2 \delta + \sigma_2 \cos^2 \delta \tag{141}$$

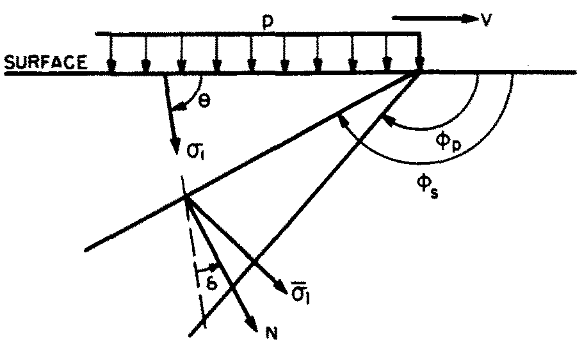

Fig. A2

Equating equations (128)–(140), and (129)–(141), gives two equations for the four unknowns $\Delta\sigma$, σ_1, σ_2 and δ, while the yield relation, $F = 0$, furnishes a third equation. The three equations are homogeneous in $\Delta\sigma$ and σ_1, σ_2 so that δ, γ, θ the stress ratios $\sigma_i/\Delta\sigma$, and their equivalent β can be computed. One finds

$$\beta = \sqrt{\left\{3\left[12\alpha^2\left(\frac{1+\nu}{1-2\nu}\right)^2 - 1\right]\right\}} \tag{142}$$

where the positive root is to be used. (The negative root corresponds only to a trivial interchange between σ_1 and σ_2.)

The principal stress deviator s_1 and the invariant J_1 are

$$s_1(\varphi_S^{(+)}) = \frac{(1-2\nu)(\beta+1)}{6(1-\nu)}\Delta\sigma \tag{143}$$

$$J_1 = \frac{(1+\nu)}{(1-\nu)}\Delta\sigma \tag{144}$$

where $\Delta\sigma$ is the as yet arbitrary stress discontinuity at φ_P, while δ is obtained from the equation

$$\cos 2\delta = \frac{3}{\beta}\cos 2(\varphi_P - \varphi_S). \tag{145}$$

Excluding the trivial addition of multiples of π, there are two roots $\pm|\delta|$ such that there are two possible values, each, for γ and θ:

$$\gamma = \frac{\pi}{2} \mp |\delta| \tag{146}$$

$$\theta = \varphi_S - \frac{\pi}{2} \pm |\delta|. \tag{147}$$

APPENDIX C

ANALYSIS FOR RANGE IIa

Solutions in this range have an inelastic pressure front, but are otherwise entirely elastic.

The stresses in the region $\bar{\varphi}^{(+)} \leq \varphi < \varphi_S$, Fig. A3, may be obtained from Section 2.2.

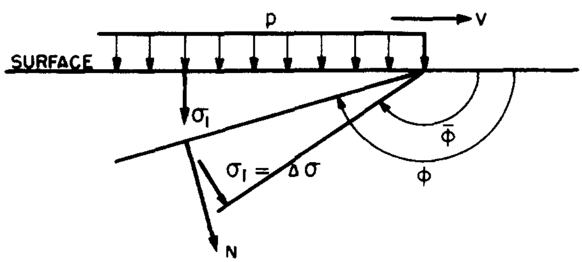

FIG. A3

Let $\Delta\sigma$ be the as yet unknown discontinuity at $\bar{\varphi}$, then one finds

$$\bar{\sigma}_1 = \Delta\sigma \qquad \bar{\sigma}_2 = \bar{\sigma}_3 = \bar{R}\Delta\sigma \tag{148}$$

where

$$\bar{R} = \frac{1-\alpha\sqrt{3}}{1+2\alpha\sqrt{3}}. \tag{149}$$

In the region $\varphi \geq \varphi_S^{(+)}$ the principal stress $\sigma_1 = -1$ is vertical; the stress $\sigma_3 = \sigma_z$ must equal $\bar{\sigma}_3$ while σ_2 remains to be determined, or

$$\sigma_1 = -1 \qquad \sigma_2 = R\sigma_1 = -R \qquad \sigma_3 = \bar{R}\Delta\sigma \tag{150}$$

where R is unknown. (The possibility of $\sigma_2 = -1$ being vertical would be a trivial interchange of subscripts.)

At the shear front, the normal and tangential stresses σ_N and σ_T must be continuous, which gives two equations to determine the unknown quantities $\Delta\sigma$ and R,

$$\Delta\sigma = -\frac{\cos 2\varphi_S}{(1-\bar{R})\cos^2(\bar{\varphi}-\varphi_S)+(1+\bar{R})\cos^2\varphi_S-1} \tag{151}$$

$$R = -1-(1+\bar{R})\Delta\sigma. \tag{152}$$

To check the condition $F \leq 0$ for $\pi > \varphi \geq \varphi_S^{(+)}$ the invariants can now be determined using equations (150), (152).

$$\left.\begin{aligned} J_1 &= (1+2\bar{R})\Delta\sigma \\ J_2 &= 1+(1+\bar{R})\Delta\sigma+\left(\frac{1+\bar{R}+\bar{R}^2}{3}\right)(\Delta\sigma)^2 \end{aligned}\right\}. \tag{153}$$

After manipulations the condition $F \leq 0$ may be brought into the form

$$\sin(4\varphi_S-2\bar{\varphi})\sin 2\bar{\varphi} \leq 0 \tag{154}$$

or, due to $\sin 2\bar{\varphi} < 0$,

$$\sin(4\varphi_S-2\bar{\varphi}) \geq 0\,. \tag{155}$$

APPENDIX D

ANALYSIS FOR RANGE III

It was concluded in Section 3 that solutions without initial discontinuities exist in Range III. Such solutions start at $\varphi = \bar{\varphi}$ with initial values $\beta = 3$, $\gamma = \pi/2$, for which the differential equations become singular so that their solution requires special treatment. To obtain asymptotic solutions near the singularity, the variables φ, β and γ are replaced by ε, Δ and η, respectively, defined in equations (122). The new variables are deemed to be small quantities, so that approximate equations can be obtained by retaining in each expression only the leading terms in the above quantities. However, the relative magnitudes of the three quantities are not known beforehand, requiring the retention of the leading terms in each of the variables. The determinantal equation (30) becomes

$$b_8\eta^2-\Delta^2 = b_9\varepsilon \tag{156}$$

where

$$b_8 = \frac{12\{3-(1-3\bar{X})[1-2\nu-4\alpha\sqrt{3}(1+\nu)]\}}{(1-2\bar{X})\left\{1-2\bar{X}(1-2\nu)+\alpha\frac{\sqrt{3}}{3}(1+\nu)[4+\alpha\sqrt{3}(2-3\bar{X})]\right\}} \tag{157}$$

$$b_9 = \frac{16(1+\nu)[1-2\nu+6\alpha^2(1+\nu)]\sqrt{\left[\left(\frac{V}{\bar{c}}\right)^2-1\right]}}{(1-2\nu)\left\{1-2\bar{X}(1-2\nu)+\alpha\frac{\sqrt{3}}{3}(1+\nu)[4+\alpha\sqrt{3}(2-3\bar{X})]\right\}} \tag{158}$$

$$\bar{X} = \frac{(1+\nu)(1+2\alpha\sqrt{3})^2}{3[1-2\nu+6\alpha^2(1+\nu)]}. \tag{159}$$

While b_9 is positive everywhere, b_8 is positive in Range III, considered here. Using equations (34)–(36) expressions for β' and γ' can be formed and, after changing to the new variables, lead to

$$\frac{d\eta}{d\varepsilon} = A_1\eta\frac{GL}{V}+1 \tag{160}$$

$$\frac{d\Delta}{d\varepsilon} = [B_1\Delta+B_2\eta^2]\frac{GL}{V} \tag{161}$$

where

$$A_1 = \frac{1}{3(1-2\bar{X})}\left\{\frac{-3+(1-2\bar{X})[1-2\nu-4\alpha\sqrt{3}(1+\nu)]}{1+(1-2\nu)(1-2\bar{X})}\right\} \tag{162}$$

$$B_1 = \frac{4}{3}\left[\frac{1-2\nu-\alpha\sqrt{3}(1+\nu)}{1+(1-2\nu)(1-2\bar{X})}\right] \tag{163}$$

$$B_2 = \frac{-4}{(1-2\bar{X})}\left\{\frac{3+(1-2\bar{X})[1-2\nu-2\alpha\sqrt{3}(1+\nu)]}{1+(1-2\nu)(1-2\bar{X})}\right\} \tag{164}$$

where $\bar{X}$ is given by equation (159).

The knowledge of the nondimensional stress variable Δ, equivalent to β, is not sufficient to find the stresses, and one additional relation is required. The most suitable one is obtained by adding equations (34) and (35), leading to an equation for (s_1+s_2),

$$\frac{d}{d\varepsilon}[\ln(s_1+s_2)] = C_1\frac{GL}{V} \tag{165}$$

where

$$C_1 = \frac{-4\alpha\sqrt{3}(1+\nu)[1-2\nu+\alpha\sqrt{3}(1-5\nu)-6\alpha^2(1+\nu)]}{3[1-2\nu+6\alpha^2(1+\nu)][1+(1-2\nu)(1-2\bar{X})]} \tag{166}$$

When solving the three equations (156), (160), (161) in the three unknowns η, Δ and GL/V, the first two are small quantities, while GL/V must go to infinity in the limit $\varepsilon \to 0$. (The possibility of finite values for this limit has been previously eliminated in Section 3 as permitting only trivial solutions $s_j = J_1 \equiv 0$.)

b_8 and b_9 being positive, equation (156) is hyperbolic in character, and permits two types of asymptotic solutions. In solutions of Type A, η and Δ are proportional to $\sqrt{\varepsilon}$,

$$\eta = \bar{D}_1\sqrt{\varepsilon} \qquad \Delta = \bar{D}_2\sqrt{\varepsilon} \tag{167}$$

while for solutions of Type B, η is proportional to $\sqrt{\varepsilon}$, while Δ is small of higher order,

$$\eta = D_1\sqrt{\varepsilon} \qquad \Delta = D_2\varepsilon^N \tag{168}$$

where $N > \frac{1}{2}$.

For solutions of Type A, equations (167), the leading terms on the right side of equations (160), (161) only are retained, giving

$$\frac{d\eta}{d\varepsilon} = A_1\eta\frac{GL}{V} \tag{169}$$

$$\frac{d\Delta}{d\varepsilon} = B_1\Delta\frac{GL}{V}. \tag{170}$$

Elimination of GL/V and substitution of equation (167) leads to a requirement on the coefficients, $A_1 = B_1$. This requirement is not satisfied, so that solutions of Type A are impossible.

To obtain solutions of Type B, only the term $b_8\eta^2$ on the left side of equation (156) is retained, so that

$$D_1 = \pm\sqrt{\left(\frac{b_9}{b_8}\right)}. \tag{171}$$

Equation (169) applies again, giving

$$\frac{GL}{V} = \frac{1}{2A_1\varepsilon}. \tag{172}$$

This relation gives the proper sign for L and satisfies the requirement for singularity of GL/V. To determine the quantity Δ it is noted that equation (170) would apply if N lies in the range $\frac{1}{2} < N < 1$ for the exponent, so that in this case again no solutions can exist. Alternatively, assuming $N > 1$, substitution of η and GL/V gives a solution for Δ proportional to ε, equivalent to $N = 1$, which is a contradiction. This leaves solely the possibility $N = 1$, for which case equation (161) indeed gives without further simplification the solution

$$D_2 = \frac{B_2D_1^2}{2A_1 - B_1}. \tag{173}$$

Being proportional to ε, the quantity Δ is small compared to η, so that—as a first approximation—the relations

$$\eta \sim \pm\sqrt{\left(\varepsilon\frac{b_9}{b_8}\right)} \tag{174}$$

$$\Delta \sim 0 \tag{175}$$

may be used. Substitution of equation (172) into equation (165) gives after integration

$$(s_1 + s_2) = C_0\varepsilon^n \tag{176}$$

where C_0 is an open constant of integration, while the exponent is

$$n = \frac{C_1}{2A_1}. \tag{177}$$

Equation (175), stating $\Delta \sim 0$, implies $\beta \sim 3$, such that the ratios of the stresses must be the same as at the inelastic shock front

$$s_2 = -\tfrac{1}{2}s_1 \tag{178}$$

$$J_1 = \frac{\sqrt{3}}{2\alpha}s_1 \tag{179}$$

$$\sigma_1 = \left[1+\frac{1}{\alpha\sqrt{12}}\right]s_1 \tag{180}$$

indicating that all stresses are proportional to ε^n. It is important that this exponent, while always positive, is less than unity and usually a very small number, of the order of 1/100 (for the specific case $\nu = 0$, $\alpha = 0{\cdot}05$ one finds $n = 0{\cdot}00598$). The derivative of the stresses with respect to the angle φ is infinite for $\varepsilon \to 0$, and the small value of n indicates a very rapid stress rise adjacent to the singularity.

(*Received* 20 *March* 1967)

Абстракт—Исследуется для упруго-пластичного материала двухмерная стационарная задача эффекта импульсного давления, движещегося с сверхсейсмической скоростью по поверхности полупространства. Принятое условие пластичности является функцией первого и второго инвариантов тензора напряжений. Оно является также подходящим для зернистой среды, в которой эеупругое деформации происходят от н внутренного скольжения при условии Куломбовского трения.

Задача неотвемленно нелинейная и приводит к системе сопряженных дифференциальных уравнений, которые решаются с помощью вычислительной машины. Характер решений совершенно зависим от важных безразмерных параметров, например от числа Маха, коэффициента Пуассона и величины α, обозначающей угол внутреннего трения. Дается таблица с решениями для разных комбинацией параметров.